1 **Formation of atmospheric molecular clusters consisting of nitric acid**

2 **with ammonia, methylamine, and dimethylamine**

3

4 Dong-Ping Chen*, Wen Ma, Chun-Hong Yang, Ming Li, Zhao-Zhen Zhou, Yang Zhang, Xi-Cun

5 Wang*, Zheng-Jun Quan*

6

7 31 pages, 11 figures, and 6 tables

8 Contents

27

28

29

ACDC model. ACDC program is used to compute the time evolution of evaporation rates, formation rates, and growth paths of the atmospheric clusters. The code can be used to solve the birth−death equations with calculated free energies (based on the QM method) as the inputs. The overall process accounts for all possible collisions and evaporation of the relevant clusters. Specifically, the birth−death equation is written as molecular clusters were calculated by considering the detailed balance in the $i + j$ reactions,[1] where i or j can be either single molecules or molecular clusters. In equilibrium, the evaporation rate is equal to the cluster formation rate:

$$i + j \leftrightarrows (i+j) \qquad\qquad 1$$

$$\gamma C_{i+j} = \beta_{ij} C_i C_j \qquad\qquad 2$$

Where γ is the evaporation rate of i or j from $i + j$, β_{ij} is the collision rate of i with j, which gives the probability that the collision finally results in an $i + j$ reaction. The collision rate β_{ij} can be determined from kinetic gas theory as [2]:

$$\beta_{ij} = \left(\frac{3}{4\pi}\right)^{1/6} \left[6k_B T\left(\frac{1}{m_i} + \frac{1}{m_j}\right)\right]^{1/2} \left(V_i^{1/3} + V_j^{1/3}\right)^2 \qquad\qquad 3$$

Where m_i and m_j are the masses of i and j, and V_i and V_j are their respective volumes.

Concentrations C_{i+j}, C_i, and C_j are related by the equilibrium constant:

$$K = \frac{C_{i+j}}{C_i C_j} = \frac{k_B T}{P_{ref}} \exp\left(\frac{-\Delta G_{rea}}{k_B T}\right) \qquad\qquad 4$$

Where Pref is the reference pressure and ΔG_{real} is the Gibbs free energy of the $i + j$ reaction. Combining the equations above, we can get an expression for the evaporation rate of i or j from the cluster $i + j$:

$$\gamma = \beta_{ij} \frac{P_{ref}}{k_B T} \exp\left(\frac{\Delta G_{i+j} - \Delta G_i - \Delta G_j}{k_B T}\right) \qquad\qquad 5$$

Where ΔG_{i+j}, ΔG_i, and ΔG_j are the Gibbs free energies of the formation of clusters $i + j$, i, and j at the reference pressure (P_{ref}) of 101.3 kPa. In this study, i and j

54 are the monomer molecules to form $i + j$ clusters and the corresponding ΔG_i or ΔG_j

55 then equals zero.

56 $$J = \frac{dc_i}{dt} = \frac{1}{2}\sum_{j<i}\beta_{j,(i-j)}c_jc_{(i-j)} + \sum_j\gamma_{(i+j)\to i}c_{(i+j)} - \sum_j\beta_{i,j}c_j - \frac{1}{2}\sum_{j<i}\gamma_{i\to j}c_i + Q_i - S_i \qquad 6$$

57 where J refers to the cluster formation rate, Q_i, set to be zero in the present study,

58 is the possible other source of i. S_i represents the sink term of i.

59 **AIM analysis.** Atoms in Molecules (AIM) theory has been regarded as one of the

60 most efficient tools to explore intermolecular interactions, such as hydrogen bonds.[3-8]

61 In this study, the topological analysis of electron density at bond critical points

62 (*BCPs*), which provides evidence for the existence of the hydrogen bonds and

63 deepens the nature of the intermolecular hydrogen bond in the clusters, is analyzed

64 with the AIM methodology to discuss the interactions between the NA with R1NHR2.

65 For the investigation of the topological characteristics at *BCPs*, the electron

66 density (ρ), its Laplacian ($\nabla^2\rho$), the electronic energy density (H), the electronic

67 kinetic energy density (G), and the electronic potential energy density (V) are

68 presented in Table **S1**. As shown in **Table S1**, the electronic densities in

69 intermolecular hydrogen bonds are from 0.0664 to 0.0936 a.u., for the $(NA)(R_1NHR_2)$

70 dimers, which are in the accepted range. The value of electronic density indicates the

71 strength of the hydrogen bond.[8, 9] The larger the value of ρ, the stronger the hydrogen

72 bond is. From Table 1, we found that the order of the ρ value for the dimers is

73 $(NA)(DMA) > (NA)(MA) > (NA)(NH_3) > (NA)_2 > (DMA)_2 > (MA)_2 > (NH_3)_2$, which

74 is consistent with the O−H···N bond length in dimers (see **Figure S2**). Their

75 corresponding positive $\nabla^2\rho$ values imply the closed-shell system interactions in all

76 dimers, which are hydrogen bonding, ionic interactions, or van der Waals forces,

77 rather than a covalent bond. Their values of $\nabla^2\rho$ are also in the general range for a

78 hydrogen bond.[10, 11] The strongest and weakest hydrogen bonds are found in the

79 $(NA)(DMA)$ and $(NH_3)_2$ dimers, respectively. Furthermore, the electronic energy

80 density (H) is viewed as an important index to explore the non-covalent interaction.

81 The positive H values show that these dimers are electrostatic in closed-shell system

82 interactions, while the interaction is predominantly covalent in the case of $H < 0$. The

83 value of -G/V is used to determine whether the regions correspond to covalent or

84 noncovalent interactions. The -G/V values are larger than 1in Table 1, showing that

85 the interaction for all dimers is noncovalent. On the other hand, the smaller the value

86 of -G/V, the stronger the hydrogen bond is. Thus, the intermolecular hydrogen bond

87 interaction between NA and DMA is the strongest.

88 **NCI analysis.** The non-covalent interaction (NCI) index, which is based on the

89 relationship between the electron density and the reduced density gradient, has been

90 mentioned as an extension of AIM by Yang and coworkers.[7] As a fundamental

91 dimensionless quantity in DFT, the reduced density gradient (*RDG*) was calculated to

92 reveal the deviation from a homogeneous electron distribution:

93
$$RDG = \frac{1}{2(3\pi^2)^{1/3}} \frac{|\nabla\rho|}{\rho^{4/3}}$$

94 Where ∇ is the gradient operator and $|\nabla\rho|$ is the electronic density gradient

95 mode. According to previous studies, the NCI index is a practical tool to identify and

96 visualize the noncovalent interactions as regions of real space. Therefore, it is useful

97 to compare the ability of intermolecular hydrogen bond interactions between NA and

98 R_1NHR_2.

99 Plots of the RDG vs. the electron density (ρ) multiplied by the sign of the second

100 Hessian eigenvalue (λ_2) for the $(NA)_2$, $(NH_3)_2$, $(MA)_2$, $(DMA)_2$, $(NA)(NH_3)$,

101 $(NA)(MA)$, and $(NA)(DMA)$ dimers are shown in **Figure S3** and **Figure 2** using the

102 Multiwfn program[12]. The reduced gradient spikes in the low densities indicate the

103 existence of the stabilizing interactions of noncovalent bonding. For the $(NA)_2$ cluster,

104 there is only one low-reduced gradient spike at low density of the sign(λ_2)ρ value of -

105 0.038 a.u., showing a stable and stronger hydrogen bond interaction. From the $(NH_3)_2$

106 to $(MA)_2$, and to $(DMA)_2$ clusters, there are only one, three, and two low-reduced

107 gradient spikes at low density of the sign(λ_2)ρ value of -0.012, -0.0065, -0.0085,

108 -0.015, -0.008. and -0.012 a.u., respectively, showing the relatively stable van der

109 Waals force interactions in the interior of these homogeneous clusters. For the

110 $(NA)(NH_3)$ dimer, there are two low-reduced gradient spikes at low density of the

111 sign(λ_2)ρ value of -0.012 and -0.068 a.u., showing a stable van der Waals force and a

112 stronger hydrogen bond interaction between NA and NH_3, respectively. For the

113 (NA)(MA) dimer, there are two low-reduced gradient spikes at low density of the

114 sign(λ_2)ρ value of -0.008 and -0.081 a.u., showing a stable van der Waals force and a

115 stronger hydrogen bond interaction between NA and MA. For the (NA)(DMA) dimer,

116 there are also two low-reduced gradient spikes at low density of the sign(λ_2)ρ value of

117 -0.008 and -0.092 a.u., showing a stable van der Waals force and a stronger hydrogen

118 bond interaction between NA and DMA. From the (NA)(NH_3) to (NA)(MA), and to

119 (NA)(DMA) dimers, the characteristic peaks directed toward the sign(λ_2)ρ values are

120 very near zero, which are -0.068, -0.081 and -0.092 a.u., respectively, indicative of

121 the relatively stronger hydrogen bond interactions between the NA and the NH_3, MA

122 or DMA. The characteristic peaks directed toward sign(λ_2)ρ values larger, then the

123 hydrogen bond interaction is weaker, therefore, the hydrogen bond interactions

124 become stronger from the (NA)(DMA) to (NA)(MA), and to (NA)(NH_3) clusters.

125 **Figure 2** also shows that there exists a bonding isosurface between the middle region

126 of the NA and NH_3, MA, or DMA. From the (NA)(NH_3), to (NA)(MA), and to

127 (NA)(DMA), the color coding of these bonding isosurfaces is from green to blue,

128 which demonstrates that the stability order of the hydrogen bonding interactions for

129 different dimers is (NA)(DMA) > (NA)(MA) > (NA)(NH_3) > $(NA)_2$ > $(DMA)_2$ >

130 $(MA)_2$ > $(NH_3)_2$. The reduced gradient isosurface ($s = 0.05$ a.u.) obtained by the VMD

131 program.[13]

132 **Average partial charge (δ_A) analysis.** In acid−base particles, proton transfer from

133 the acid moiety to the base moiety may take place easily, depending on the strengths

134 of the acid and the base. The proton transfer considered here is for the equilibrium

135 structure of the cluster. We define proton transfer to occur in the present context if the

136 average partial charges (δ_A) on the acid and base moieties are at least of magnitude

137 0.5. (In fact, for the systems studied the typical values of δ_A in the case of proton

138 transfer are of the order of $0.8 \sim 0.9$; there are no borderline cases; In this article, δ_A

139 refers to the average partial charge on the base groups). The average partial charges

140 (δ_A) at M06-2X/6-31++G(d,p) level were calculated using natural bond orbital (NBO)

141 analysis.[14, 15]

142   For the most stable structure $(NA)_n(R_1NHR_2)_m$ ($1 \leq m$, $n \leq 4$) clusters, except

143    $(NA)(R_1NHR_2)$ and $(NA)(NH_3)_2$ clusters in **Table S2**, all protons are complete

144   transferred from NA to R_1NHR_2. In $(NA)(NH_3)$, $(NA)(MA)$, $(NA)(DMA)$ and

145    $(NA)(NH_3)_2$ clusters, a pronounced proton transfer was not involved ($\delta_A = 0.116$,

146   0.137, 0.157 and 0.169, respectively), thus ion pair $(NO_3)^-(R_1NHR_2)^+$ are not formed

147   which can be deduced by both the proton location and the average partial charge. The

148   small δ value in this case ($\delta_A < 0.2$) does not correspond to proton transfer. In other

149   clusters, there are one or more hydrogen bonds connecting NA to R_1NHR_2, in which

150   NA acts as the hydrogen-bond donor, and R_1NHR_2 is the acceptor. The occurrence of

151   proton transfer affects the binding energy since the proton-transfer complexes are

152   bonded ionically, rather than by (neutral) hydrogen bonding. For $(NA)_m(R1NHR2)$ (m

153    $= 2 \sim 4$) and $(NA)(R_1NHR_2)_n$ ($n = 2 \sim 4$) clusters except for $(NA)(NH_3)_2$ cluster, the

154   average partial charge δ_A on R_1NHR_2 is in a range of $0.804 \sim 0.891$. From NH_3 to

155   DMA, δ_A is increased gradually. The same as above, for $(NA)_m(R_1NHR_2)_n$ ($2 \leq m$, $n \leq$

156   4) clusters, the average partial charge δ_A on R_1NHR_2 is in a range of $0.807 \sim 0.890$.

157   Larger δ_A values (> 0.8) indicate that protons on NA are completely transferred to

158   R_1NHR_2 molecules and it also means that hydrogen bonds and electrostatic forces

159   become stronger, which are conducive to the stability of clusters. This stability against

160   dissociation is favorable for particle growth.

161   **Boundary condition.** The boundary conditions require that the outgrowing clusters

162   are stable enough and the clusters are more likely to grow than to evaporate. For

163    $(NA)_m(R_1NHR_2)_n$ ($0 \leq m$, $n \leq 4$) clusters, the clusters with approximately equal

164   numbers of acid and base molecules or number of acid molecules one greater than that

165   of R_1NHR_2 molecules have low evaporation rates and high concentrations in the

166   simulations. This allows us to assume that $(NA)_5(R_1NHR_2)_5$ and $(NA)_4(R_1NHR_2)_5$ are

167   stable enough and do not evaporate. Therefore, in the ACDC simulation,

168    $(NA)_5(R_1NHR_2)_5$ and $(NA)_4(R_1NHR_2)_5$ that can be formed via a collision between

169   small clusters or evaporation from larger clusters in the simulation are allowed to

170   leave the simulation box. Similarly, for $(SA)_m(NH_3)_n$ ($0 \leq m$, $n \leq 4$), $(SA)_m(MA)_n$ ($0 \leq$

171   m, $n \leq 3$) and $(SA)_m(DMA)_n$ ($0 \leq m$, $n \leq 4$), $(SA)_5(NH_3)_5$ and $(SA)_4(NH_3)_5$,
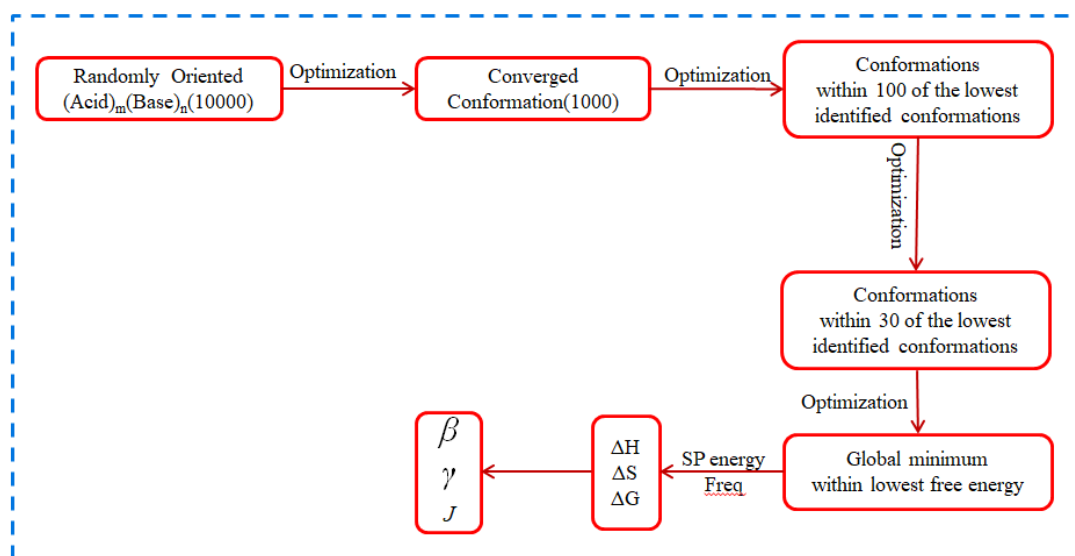
172 $(SA)_4(MA)_4$ and $(SA)_3(MA)_4$, and $(SA)_5(DMA)_5$ $(SA)_4(DMA)_5$ are allowed to leave

173 the simulation box. All other clusters crossing the box edge for H_2SO_4–NH_3,

174 H_2SO_4–MA, and H_2SO_4–DMA systems are brought back to the simulation by

175 monomer evaporations.

176 **Stability of clusters.** In the process of acid–base cluster growth, a cluster can be

177 considered to be stable when collisions with monomers or other clusters occur before

178 evaporation. In other words, a cluster can be considered to be stable if its collision

179 rate with acid, base monomer, or other clusters is higher than its evaporation rate of

180 the cluster. In general, the collision rate constant of a cluster with acid or base

181 monomer is of the order of 10^{-10} cm^3 s^{-1}. When the concentration of acid or base

182 monomer is at ppt level, the collision rate of the cluster with acid or base monomer

183 can reach about 10^{-1} s^{-1}. Therefore, we consider clusters with evaporation rates lower

184 than 10^{-2} s^{-1} to be stable.

185 **Hydration free energies.** The calculated Gibbs free energies (ΔG_{ref}) of hydration at

186 298.15 K and 1 atm are presented in **Table S5**. The corresponding enthalpy of

187 hydration (ΔH) and entropy of hydration (ΔS) are presented in **Table S6**, and the

188 optimized geometries are shown in **Figure S10**. As shown in **Table S5**, hydration-free

189 energies for all pure R_1NHR_2 and pure NA clusters are all negative. For the addition

190 of the first water molecule, hydration-free energies for all hetero-molecular clusters

191 $(NA)_m(R_1NHR_2)_n$ ($0 \leq m, n \leq 2$) are negative with $(NA)_2(NH_3)_2$ being the most

192 favorable one. A proton transfer is induced between the NA and R_1NHR_2 molecules

193 when adding water molecules to the cluster (see **Figure S2** and **Figure S10**,

194 respectively), which explains the evaporation rate of $(NA)(R_1NHR_2)$ cluster decreases

195 with the increase of RH. The addition of water molecules to a cluster with an equal

196 number of NA and R_1NHR_2 molecules is more favorable than to other clusters. For

197 the addition of the last H_2O molecule, the hydration-free energies for all hetero-

198 molecular clusters $(NA)_m(R_1NHR_2)_n$ ($0 \leq m, n \leq 2$) are positive or close to zero.

199 Hence, the addition of a last H_2O molecule to any cluster is not favorable. This is

200 consistent with previous findings that the addition of more water molecules leads to a
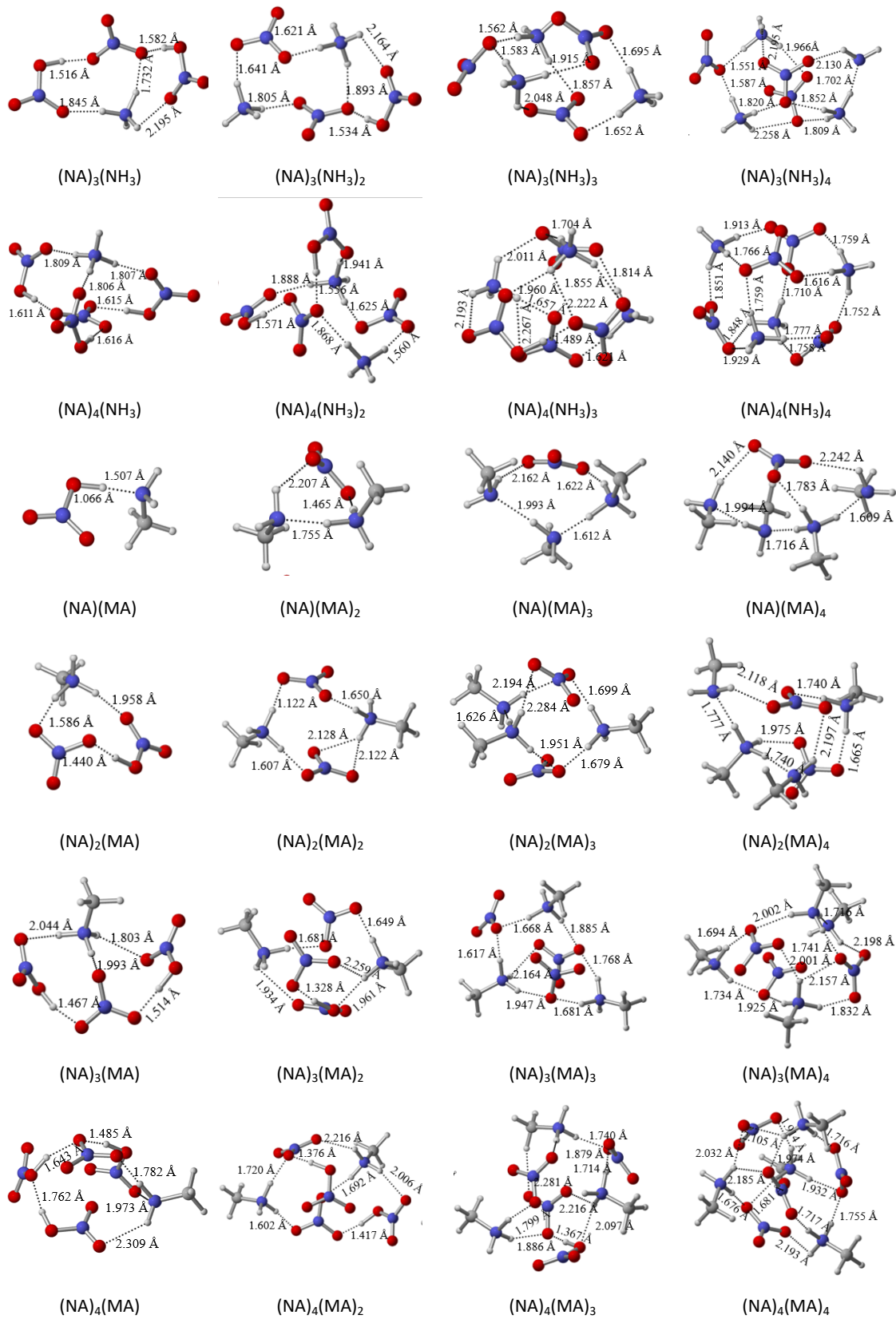
201 decrease in hydration-free energies.

202　　　Based on the calculated hydration–free energies, the hydrate distribution of the

203　clusters was calculated at relative humidity (RH) 20%, 40%, 60%, and 80%, at 278.15

204　K. As shown in **Figure S11**, dry clusters for the pure R_1NHR_2 cluster constitute

205　almost 100% of the population at all considered RH conditions. Therefore, pure

206　R_1NHR_2 clusters are not hydrated at atmospheric conditions. At low RH of 20% and

207　278.15 K, dry clusters are predominantly populated for the R_1NHR_2 molecule and

208　$(R_1NHR_2)_2$ cluster, but to other hetero-molecular clusters on the contrary. With

209　increasing RH, dominant hydration distribution for NA molecule and $(NA)_2$ cluster

210　gradually transfers to multi-hydrate. For $(NA)(NH_3)$, $(NA)_2(NH_3)$, $(NA)(NH_3)_2$, and

211　$(NA)_2(NH_3)_2$ clusters, RH has little effect on distribution, dominant hydration

212　distribution mainly tetra-hydrate, tetra-hydrate, tri-hydrate and hepta-hydrate,

213　respectively. Similar to above, for $(NA)(MA)_2$, $(NA)_2(MA)$, $(NA)_2(MA)_2$,

214　$(NA)(DMA)$, $(NA)(DMA)_2$ and $(NA)_2(DMA)_2$ clusters dominant hydration

215　distribution all mainly tri-hydrate. As an exception $(NA)_2(NH_3)_2$, $(NA)(MA)$ and

216　$(NA)_2(DMA)$ clusters, the high-hydrate form populates more than 60% of the

217　distribution at all considered RH conditions. In addition, clusters with the last H_2O

218　molecules have a negligible population at all considered RH conditions. These

219　findings generally show that the NA–R_1NHR_2 clusters are strongly hydrated,

220　especially for $(NA)_2(NH_3)_2$, $(NA)(MA)$, and $(NA)_2(DMA)$ clusters.

221

222

**Figure S1.** Flowchart for the multistep global minimum sampling method.

0.973 Å

NA

1.767 Å

(NA)$_2$

1.837 Å   1.794 Å   1.780 Å

(NA)$_3$

1.714 Å   1.714 Å   1.714 Å   1.714 Å

(NA)$_4$

1.014 Å

NH$_3$

2.424 Å

(NH$_3$)$_2$

2.162 Å

(NH$_3$)$_3$

2.097 Å

(NH$_3$)$_4$

1.014 Å

MA

2.240 Å

(MA)$_2$

2.202 Å   2.235 Å   2.144 Å

(MA)$_3$

2.178 Å   2.084 Å   3.081 Å   2.104 Å

(MA)$_4$

1.015 Å

DMA

2.418 Å   1.018 Å

(DMA)$_2$

2.197 Å   2.158 Å   1.022 Å   2.197 Å

(DMA)$_3$

2.148 Å   2.149 Å   2.147 Å   2.147 Å

(DMA)$_4$

1.042 Å   1.576 Å

(NA)(NH$_3$)

2.204 Å   1.985 Å   1.097 Å   1.446 Å

(NA)(NH$_3$)$_2$

1.507 Å   2.244 Å   1.662 Å   2.046 Å

(NA)(NH$_3$)$_3$

2.015 Å   2.170 Å   1.611 Å   2.076 Å   1.764 Å   1.864 Å

(NA)(NH$_3$)$_4$

1.865 Å   1.477 Å   1.461 Å

(NA)$_2$(NH$_3$)

1.592 Å   1.756 Å   1.756 Å   1.592 Å

(NA)$_2$(NH$_3$)$_2$

1.666 Å   1.770 Å   2.222 Å   1.756 Å   1.949 Å   2.379 Å   1.557 Å

(NA)$_2$(NH$_3$)$_3$

1.747 Å   1.709 Å   2.277 Å   2.271 Å   1.931 Å   1.932 Å   2.277 Å   2.271 Å   1.709 Å   1.747 Å

(NA)$_2$(NH$_3$)$_4$

(NA)₃(NH₃)　　(NA)₃(NH₃)₂　　(NA)₃(NH₃)₃　　(NA)₃(NH₃)₄

(NA)₄(NH₃)　　(NA)₄(NH₃)₂　　(NA)₄(NH₃)₃　　(NA)₄(NH₃)₄

(NA)(MA)　　(NA)(MA)₂　　(NA)(MA)₃　　(NA)(MA)₄

(NA)₂(MA)　　(NA)₂(MA)₂　　(NA)₂(MA)₃　　(NA)₂(MA)₄

(NA)₃(MA)　　(NA)₃(MA)₂　　(NA)₃(MA)₃　　(NA)₃(MA)₄

(NA)₄(MA)　　(NA)₄(MA)₂　　(NA)₄(MA)₃　　(NA)₄(MA)₄

Figure S2. Optimized stable structures of dimers and $(NA)_n(R_1NHR_2)_m$ clusters ($0 \leq m$, $n \leq 4$). Red, blue, gray, and light gray spheres represent oxygen, nitrogen, carbon, and hydrogen atoms, respectively. Dashed lines and numbers indicate the formation of hydrogen bonds and bond length (in angstroms), respectively.

229
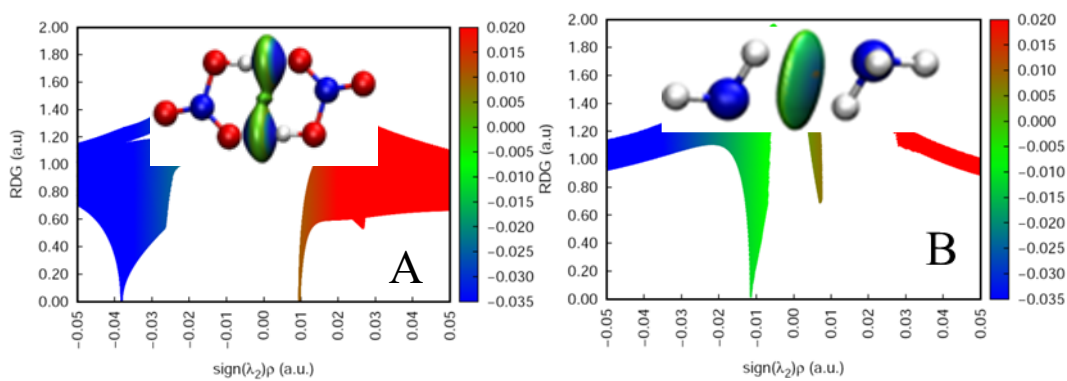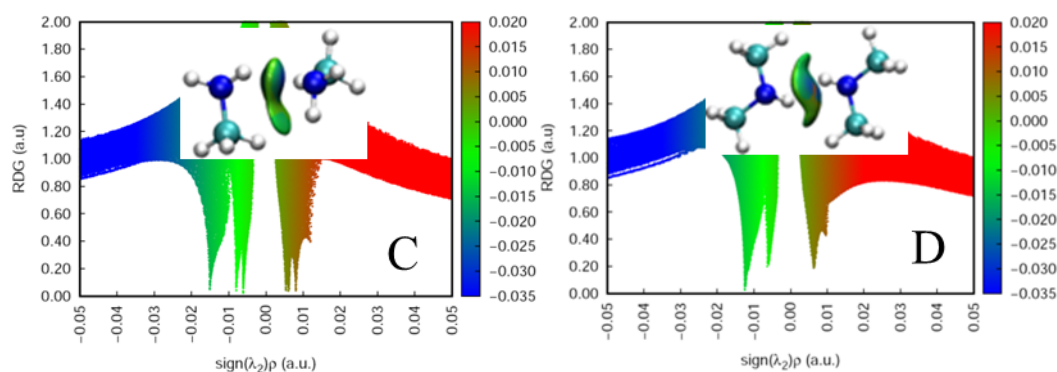
Figure S3. Noncovalent interactions (NCI) analysis among the global minima for (NA)$_2$ (A),
(NH$_3$)$_2$ (B), (MA)$_2$ (C), (DMA)$_2$ (D).

232
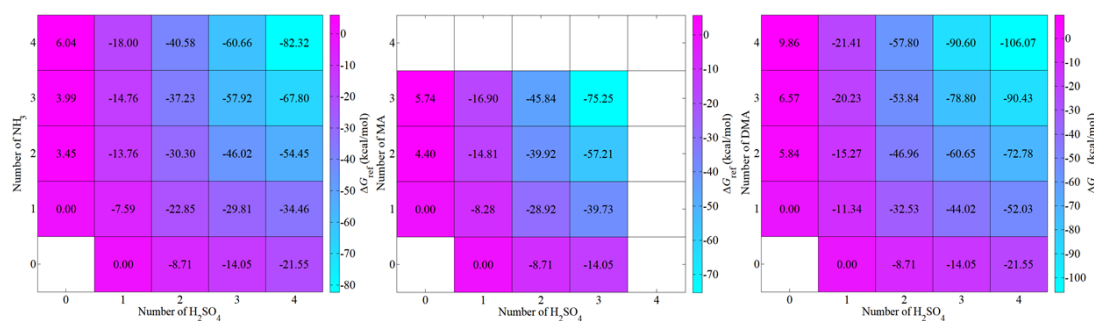
Figure S4. Calculated formation free energies for (SA)$_m$(R$_1$NHR$_2$)$_n$ (0 ≤ m, n ≤ 3 (4), left panel
for NH$_3$, middle panel for MA, right panel for DMA) at the DLPNO-CCSD(T)/ aug-cc-
pVTZ//M06-2X/6-31++G(d,p) level and 298.15 K and 1 atm (reference pressure of acid and base).

236

237
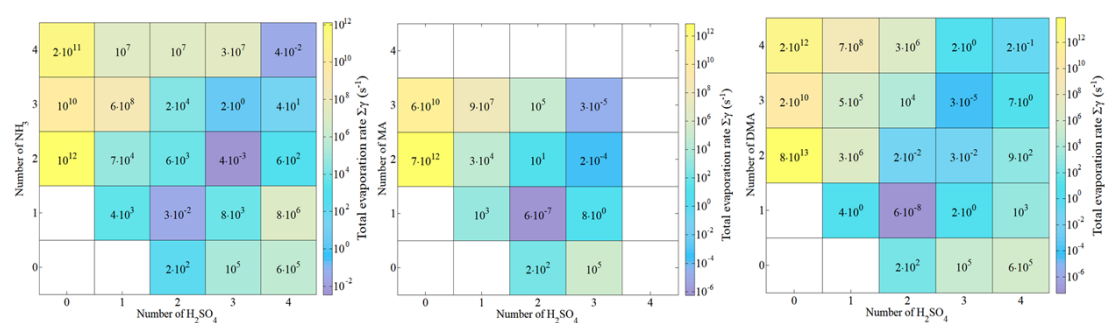
Figure S5. The evaporation rates for (SA)$_m$(R$_1$NHR$_2$)$_n$ (0 ≤ m, n ≤ 3 (4), left panel for NH$_3$,
middle panel for MA, right panel for DMA) on the base−SA grid at 278.15.

12
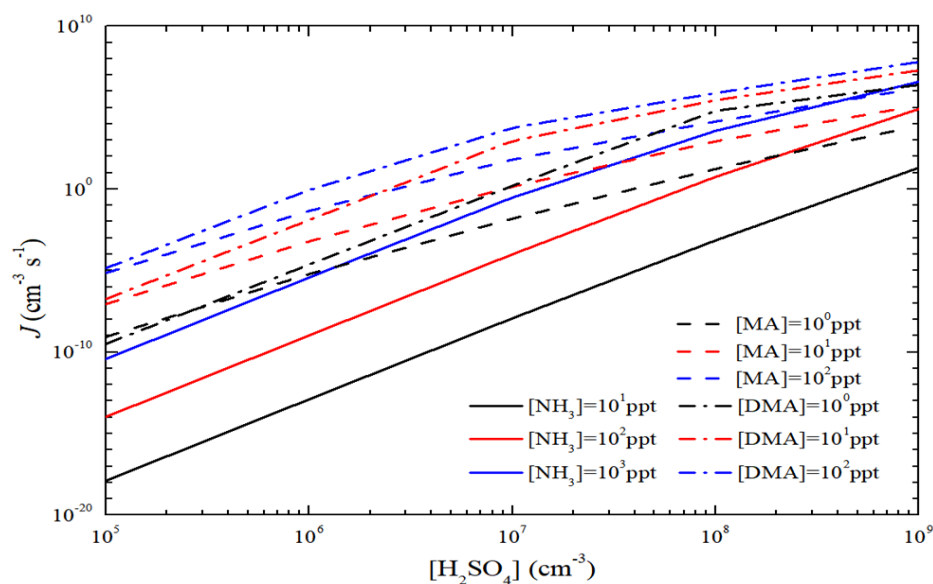
Figure S6. The cluster formation rate J (cm^{-3} s^{-1}) out of the simulation (SA)$_m$(R$_1$NHR$_2$)$_n$ system as a function of monomer concentration at 278.15 K.
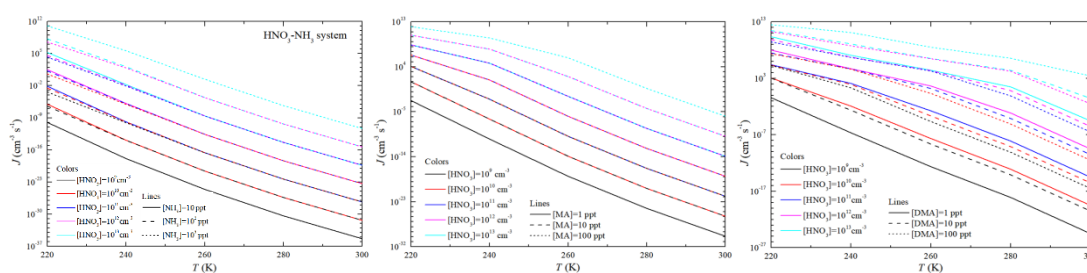
Figure S7. Simulated cluster formation rate J out of the simulation (NA)$_m$(R$_1$NHR$_2$)$_n$ system as a function of temperature.
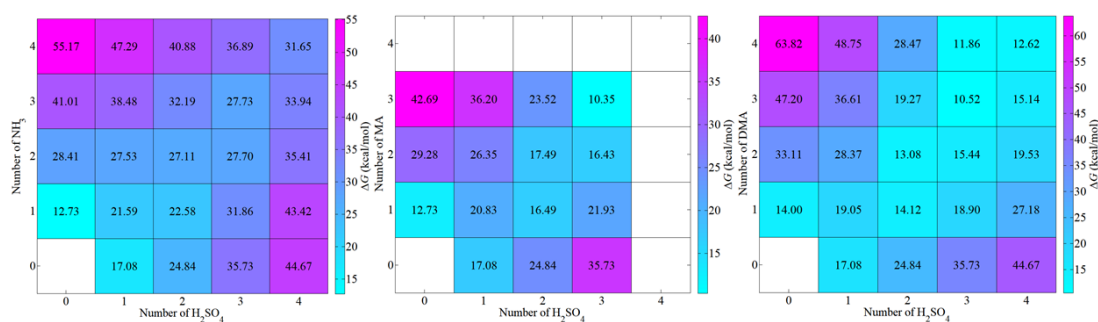
Figure S8. Actual Gibbs free energy surface for the formation of clusters (SA)$_m$(R$_1$NHR$_2$)$_n$ (right for NH$_3$, middle for MA, left for DMA) at 278.15 K, [SA] = 10^6 cm^{-3}, [NH$_3$] = 10^2 ppt and [MA] = [DMA] = 10 ppt.

250
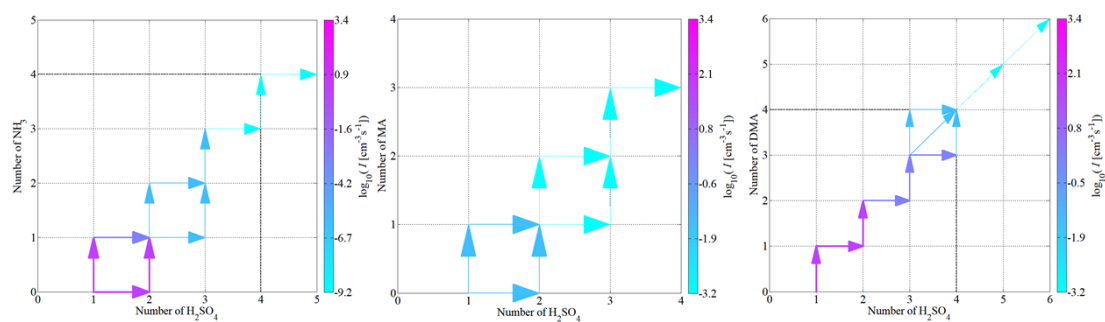
Figure S9. Main clustering pathways for the formation of clusters $(SA)_m(R_1NHR_2)_n$ (right for NH_3, middle for MA, left for DMA) at 278.15 K, $[SA] = 10^6$ cm^{-3}, $[NH_3] = 10^2$ ppt and $[MA] = [DMA] = 10$ ppt. For figure clarity, the pathways contributing less than 5% to the flux of the cluster are not shown.

| (NA)W | (NA)W$_2$ | (NA)W$_3$ | (NA)$_2$W |

| (NA)$_2$W$_2$ | (NA)$_2$W$_3$ | (NH$_3$)W | (NH$_3$)W$_2$ |

| (NH$_3$)W$_3$ | (NH$_3$)$_2$W | (NH$_3$)$_2$W$_2$ | (NH$_3$)$_2$W$_3$ |

| (NA)(NH$_3$)W | (NA)(NH$_3$)W$_2$ | (NA)(NH$_3$)W$_3$ | (NA)(NH$_3$)W$_4$ |
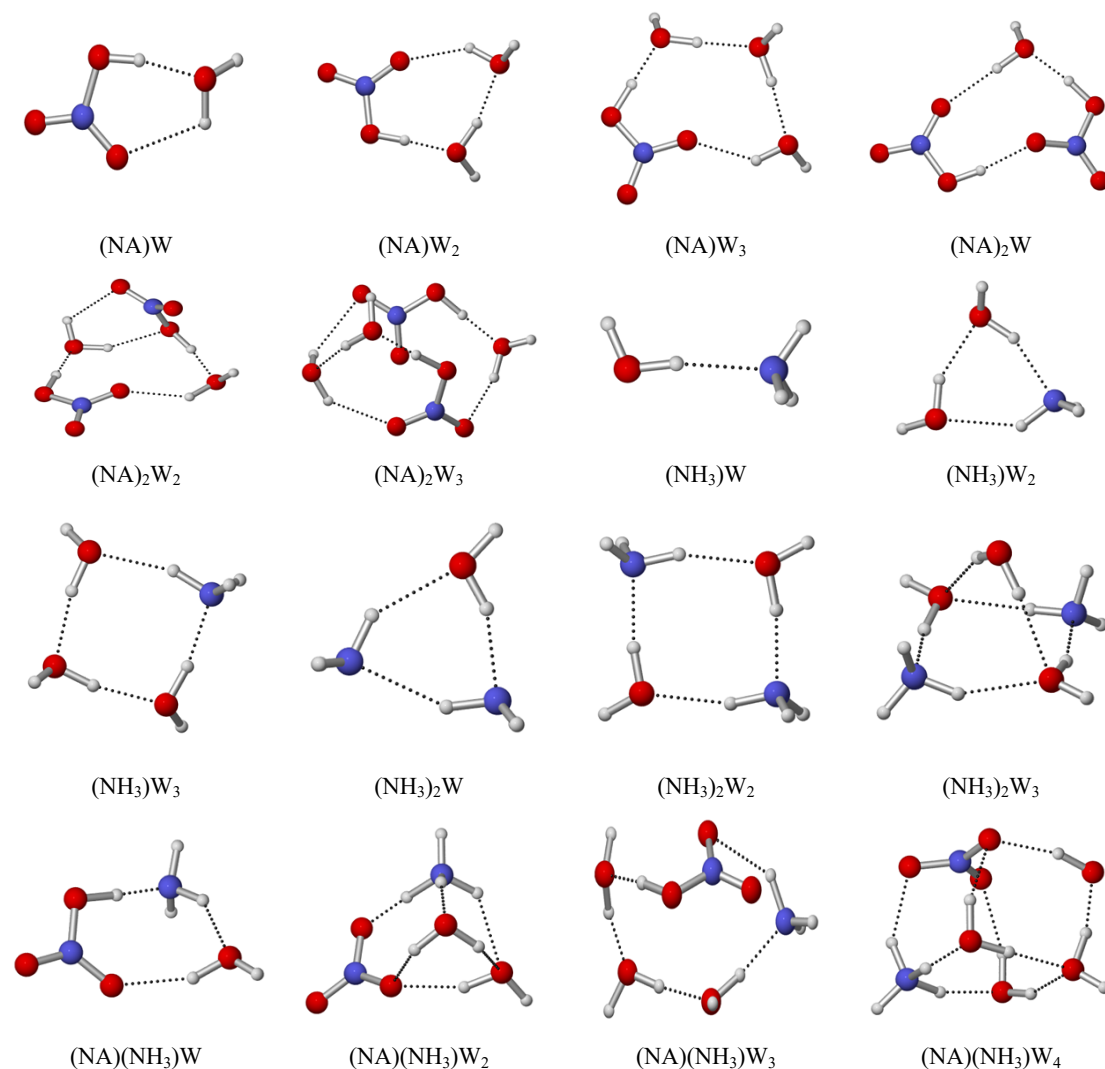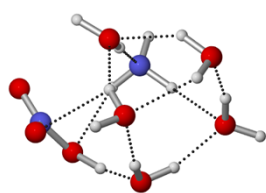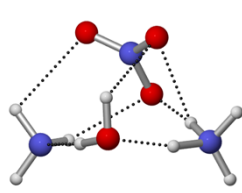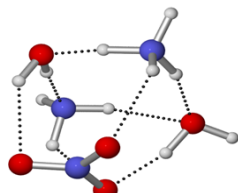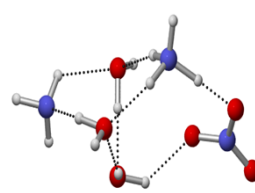
(NA)(NH₃)W₅   (NA)(NH₃)₂W   (NA)(NH₃)₂W₂   (NA)(NH₃)₂W₃
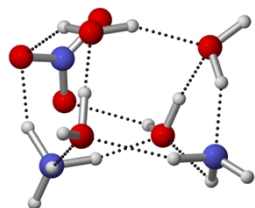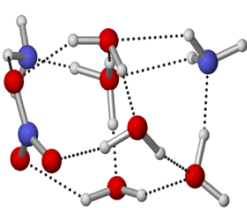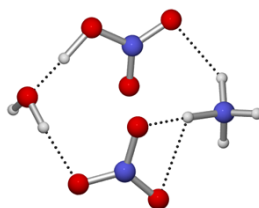
(NA)(NH₃)₂W₄   (NA)(NH₃)₂W₅   (NA)₂(NH₃)W   (NA)₂(NH₃)W₂
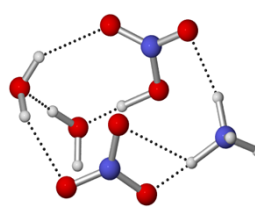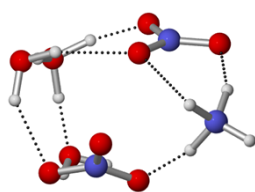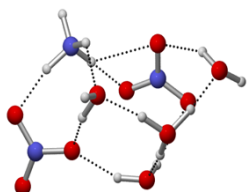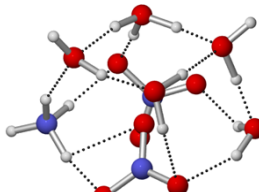
(NA)₂(NH₃)W₃   (NA)₂(NH₃)W₄   (NA)₂(NH₃)W₅   (NA)₂(NH₃)₂W
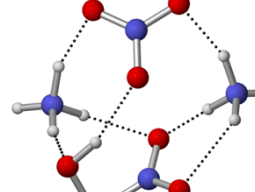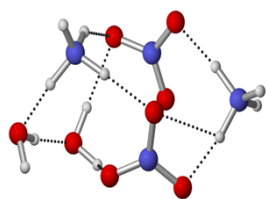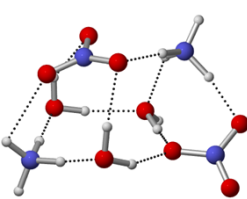
(NA)₂(NH₃)₂W₂   (NA)₂(NH₃)₂W₃   (NA)₂(NH₃)₂W₄   (NA)₂(NH₃)₂W₅
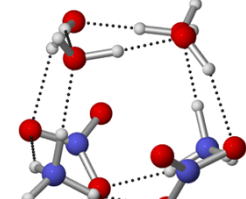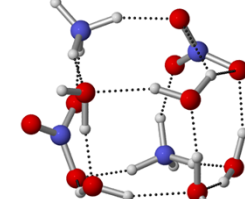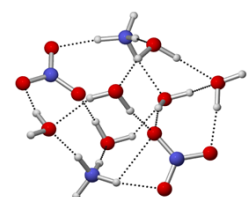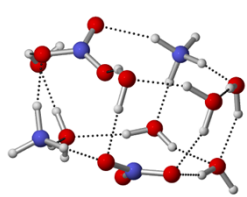
(NA)₂(NH₃)₂W₆   (NA)₂(NH₃)₂W₇   (NA)₂(NH₃)₂W₈   (MA)W
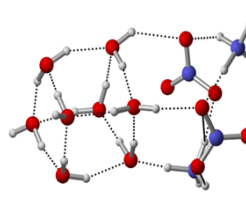
(MA)W₂   (MA)W₃   (MA)₂W   (MA)₂W₂

15

(MA)₂W₃   (NA)(MA)W   (NA)(MA)W₂   (NA)(MA)W₃

(NA)(MA)W₄   (NA)(MA)W₅   (NA)(MA)W₆   (NA)(MA)W₇

(NA)(MA)₂W   (NA)(MA)₂W₂   (NA)(MA)₂W₃   (NA)(MA)₂W₄

(NA)₂(MA)W   (NA)₂(MA)W₂   (NA)₂(MA)W₃   (NA)₂(MA)W₄

(NA)₂(MA)₂W   (NA)₂(MA)₂W₂   (NA)₂(MA)₂W₃   (NA)₂(MA)₂W₄

(DMA)W   (DMA)W₂   (DMA)W₃   (DMA)₂W

$(MA)_2W_3$ $(NA)(MA)W$ $(NA)(MA)W_2$ $(NA)(MA)W_3$

$(NA)(MA)W_4$ $(NA)(MA)W_5$ $(NA)(MA)W_6$ $(NA)(MA)W_7$

$(NA)(MA)_2W$ $(NA)(MA)_2W_2$ $(NA)(MA)_2W_3$ $(NA)(MA)_2W_4$

$(NA)_2(MA)W$ $(NA)_2(MA)W_2$ $(NA)_2(MA)W_3$ $(NA)_2(MA)W_4$

$(NA)_2(MA)_2W$ $(NA)_2(MA)_2W_2$ $(NA)_2(MA)_2W_3$ $(NA)_2(MA)_2W_4$

$(DMA)W$ $(DMA)W_2$ $(DMA)W_3$ $(DMA)_2W$

(DMA)$_2$W$_2$

(DMA)$_2$W$_3$

(NA)(DMA)W

(NA)(DMA)W$_2$

(NA)(DMA)W$_3$

(NA)(DMA)W$_4$

(NA)(DMA)$_2$W

(NA)(DMA)$_2$W$_2$

(NA)(DMA)$_2$W$_3$

(NA)(DMA)$_2$W$_4$

(NA)$_2$(DMA)W

(NA)$_2$(DMA)W$_2$

(NA)$_2$(DMA)W$_3$

(NA)$_2$(DMA)W$_4$

(NA)$_2$(DMA)W$_5$

(NA)$_2$(DMA)W$_6$

(NA)$_2$(DMA)W$_7$

(NA)$_2$(DMA)$_2$W

(NA)$_2$(DMA)$_2$W$_2$

(NA)$_2$(DMA)$_2$W$_3$

(NA)$_2$(DMA)$_2$W$_4$

255 **Figure S10.** Optimized the lowest free energy cluster structures of $(NA)_m(R_1NHR_2)_nW_x$ ($m = 1 \sim 2$,

256 $n = 0 \sim 2$ and $x = 1 \sim 8$) at M06-2X/6-31++G(d,p) level. The red balls stand for O atoms, the blue

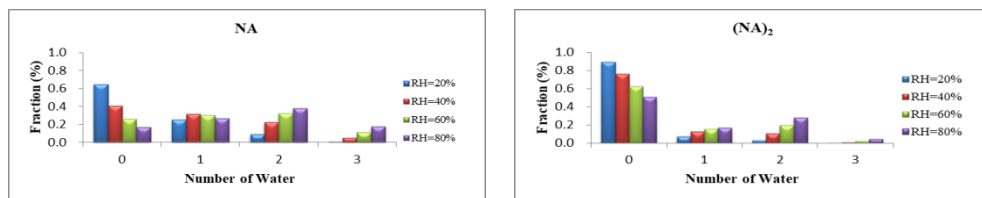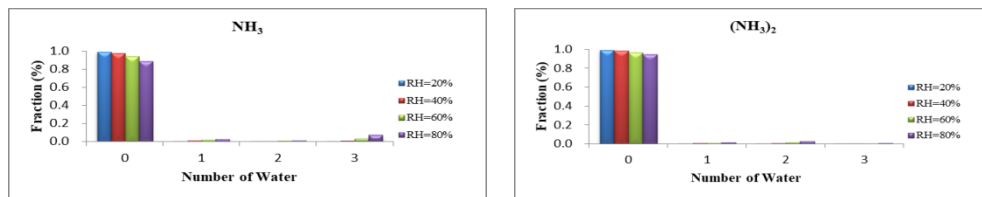257 ones for N atoms, the green ones for C atoms, and the white ones for H atoms.
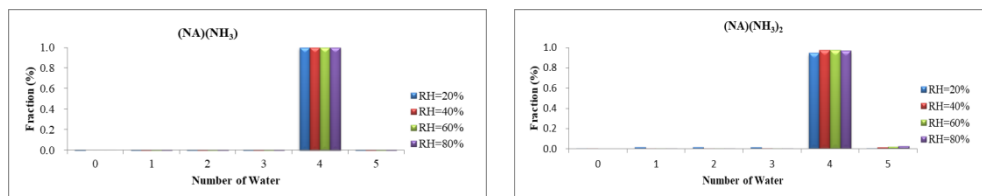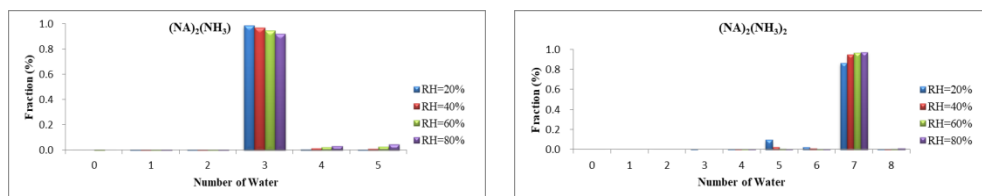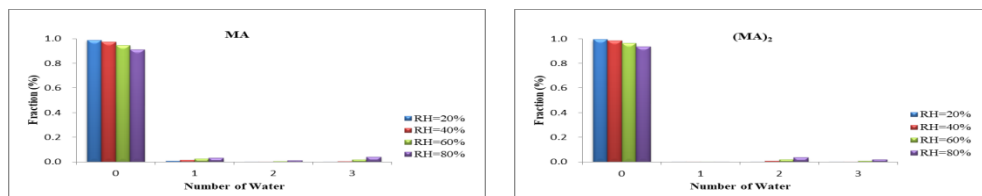
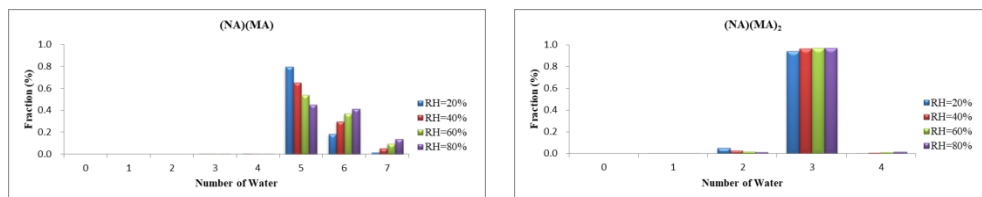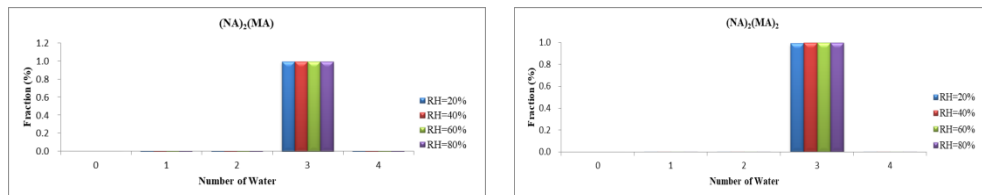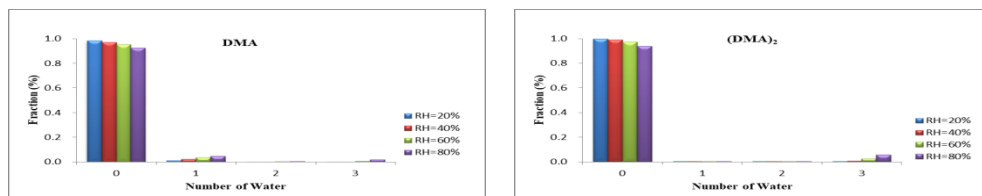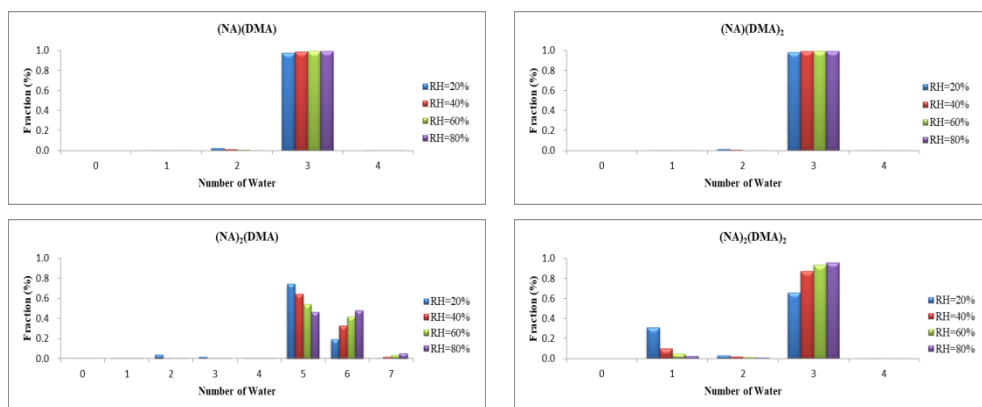**Figure S11.** Hydrate distribution of clusters for NA, $(NA)_2$, $(NA)_1(R_1NHR_2)_1$, $(NA)_1(R_1NHR_2)_2$, $(NA)_2(R_1NHR_2)_1$ and $(NA)_2(R_1NHR_2)_2$ at different relative humidity and 278.15 K.

Table S1. Topological parameters at intermolecular bond critical points (*BCP*) of all dimers at the M06-2X/6-31++G(d,p) level

Species	ρ/a.u.	$\nabla^2\rho$/a.u.	H/a.u.	G/a.u.	V/a.u.	$-G/V$
$(NA)_2$	0.0382	0.1102	-0.0055	0.0330	-0.0385	0.8571
$(NH_3)_2$	0.0115	0.0453	-0.0020	0.0094	-0.0074	1.2703
$(MA)_2$	0.0151	0.0535	0.0020	0.0114	-0.0095	1.2000
$(DMA)_2$	0.0125	0.0523	0.0021	0.0110	-0.0090	1.2222
$(NA)(NH_3)$	0.0664	0.0466	-0.0269	0.0385	-0.0654	0.5887
$(NA)(MA)$	0.0809	0.0276	-0.0378	0.0447	-0.0824	0.5425
$(NA)(DMA)$	0.0936	0.0025	-0.0486	0.0492	-0.0979	0.5026

Table S2. The Average Partial charge δ_A on R_1NHR_2 groups in $(NA)_m(R_1NHR_2)_n$ ($1 \leq m, n \leq 4$).

δ_A	1	2	3	4
	0.116	0.085	0.831	0.848
1	0.137	0.814	0.843	0.853
	0.157	0.824	0.872	0.858
	0.807	0.807	0.830	0.852
2	0.842	0.822	0.852	0.849
	0.850	0.828	0.834	0.867
	0.872	0.833	0.890	0.828
3	0.891	0.849	0.830	0.837
	0.872	0.858	0.830	0.842
	0.869	0.827	0.821	0.813
4	0.875	0.861	0.849	0.839
	0.890	0.871	0.848	0.825

[a]Row and column indices indicate m NA molecules and n R_1NHR_2 (above for NH_3, middle for MA, bottom for DMA) molecules, respectively.

276

277 **Table S3.** The thermochemical information including enthalpy ΔH (kcal/mol) and entropy ΔS (

278 cal/(mol·K)) for the studied molecular clusters at 298.15 K and 1 atm.

Species	ΔH (298.15 K)	ΔS (298.15 K)
(NA)$_2$	-9.79	-33.2
(NA)$_3$	-15.60	-69.1
(NA)$_4$	-26.74	-104.0
(NH$_3$)$_2$	-3.92	-24.7
(NH$_3$)$_3$	-13.28	-57.9
(NH$_3$)$_4$	-20.59	-89.3
(NA)(NH$_3$)	-14.53	-32.0
(NA)(NH$_3$)$_2$	-23.29	-63.7
(NA)(NH$_3$)$_3$	-34.82	-102.9
(NA)(NH$_3$)$_4$	-43.46	-131.4
(NA)$_2$(NH$_3$)	-24.22	-71.5
(NA)$_2$(NH$_3$)$_2$	-43.25	-107.4
(NA)$_2$(NH$_3$)$_3$	-56.62	-146.8
(NA)$_2$(NH$_3$)$_4$	-72.57	-173.4
(NA)$_3$(NH$_3$)	-36.91	-105.6
(NA)$_3$(NH$_3$)$_2$	-58.34	-141.8
(NA)$_3$(NH$_3$)$_3$	-77.28	-186.3
(NA)$_3$(NH$_3$)$_4$	-91.49	-219.1
(NA)$_4$(NH$_3$)	-52.39	-143.4
(NA)$_4$(NH$_3$)$_2$	-73.18	-181.4
(NA)$_4$(NH$_3$)$_3$	-97.31	-230.6
(NA)$_4$(NH$_3$)$_4$	-126.39	-267.6
(MA)$_2$	-4.14	-28.6
(MA)$_3$	-12.63	-61.6
(MA)$_4$	-19.99	-94.7
(NA)(MA)	-15.83	-34.9
(NA)(MA)$_2$	-25.46	-72.8
(NA)(MA)$_3$	-35.86	-105.2
(NA)(MA)$_4$	-45.10	-140.7
(NA)$_2$(MA)	-26.75	-72.3
(NA)$_2$(MA)$_2$	-52.35	-109.4
(NA)$_2$(MA)$_3$	-68.87	-150.4
(NA)$_2$(MA)$_4$	-82.29	-185.8
(NA)$_3$(MA)	-41.63	-113.9
(NA)$_3$(MA)$_2$	-68.67	-156.4
(NA)$_3$(MA)$_3$	-92.78	-190.0
(NA)$_3$(MA)$_4$	-107.76	-224.2
(NA)$_4$(MA)	-50.68	-151.9

$(NA)_4(MA)_2$	-83.18	-192.6
$(NA)_4(MA)_3$	-107.21	-234.7
$(NA)_4(MA)_4$	-140.61	-272.4
$(DMA)_2$	-5.01	-36.4
$(DMA)_3$	-13.87	-68.6
$(DMA)_4$	-20.46	-101.7
$(NA)(DMA)$	-16.17	-34.2
$(NA)(DMA)_2$	-27.90	-72.0
$(NA)(DMA)_3$	-36.61	-101.7
$(NA)(DMA)_4$	-49.53	-149.7
$(NA)_2(DMA)$	-31.74	-70.3
$(NA)_2(DMA)_2$	-61.01	-110.0
$(NA)_2(DMA)_3$	-72.11	-153.8
$(NA)_2(DMA)_4$	-85.03	-193.4
$(NA)_3(DMA)$	-42.69	-111.5
$(NA)_3(DMA)_2$	-76.35	-155.5
$(NA)_3(DMA)_3$	-97.78	-190.8
$(NA)_3(DMA)_4$	-112.10	-234.4
$(NA)_4(DMA)$	-56.75	-155.6
$(NA)_4(DMA)_2$	-90.59	-197.4
$(NA)_4(DMA)_3$	-114.07	-233.9
$(NA)_4(DMA)_4$	-145.18	-274.6

279

280 **Table S4.** Evaporation coefficients (s^{-1}) for all evaporation pathways of $(NA)_m(R_1NHR_2)_n$ ($0 \leq m$,

281 $n \leq 4$) clusters under study at 278.15 K.

Evaporation pathway	Evaporation coefficients
$(NH_3)_2 \rightarrow (NH_3)+(NH_3)$	1.32×10^{12}
$(NH_3)_3 \rightarrow (NH_3)_2+(NH_3)$	1.11×10^{10}
$(NH_3)_4 \rightarrow (NH_3)_3+(NH_3)$	2.01×10^{11}
$(NH_3)_4 \rightarrow (NH_3)_2+(NH_3)_2$	3.53×10^8
$(NA)(NH_3) \rightarrow (NA)_1+(NH_3)$	4.72×10^5
$(NA)(NH_3)_2 \rightarrow (NA)(NH_3)+(NH_3)$	1.55×10^{10}
$(NA)(NH_3)_2 \rightarrow (NA)+(NH_3)_2$	2.39×10^3
$(NA)(NH_3)_3 \rightarrow (NA)(NH_3)_2+(NH_3)$	5.09×10^9
$(NA)(NH_3)_3 \rightarrow (NA)(NH_3)+(NH_3)_2$	2.25×10^7
$(NA)(NH_3)_3 \rightarrow (NA)+(NH_3)_3$	9.82×10^2
$(NA)(NH_3)_4 \rightarrow (NA)(NH_3)_3+(NH_3)$	4.64×10^9
$(NA)(NH_3)_4 \rightarrow (NA)(NH_3)_2+(NH_3)_2$	6.02×10^6
$(NA)(NH_3)_4 \rightarrow (NA)(NH_3)+(NH_3)_3$	7.57×10^6
$(NA)(NH_3)_4 \rightarrow (NA)+(NH_3)_4$	2.08×10^1
$(NA)_2 \rightarrow (NA)+(NA)$	1.80×10^9
$(NA)_2(NH_3) \rightarrow (NA)_2+(NH_3)$	1.66×10^7
$(NA)_2(NH_3) \rightarrow (NA)(NH_3)+(NA)$	1.12×10^{11}

Reaction	Rate
$(NA)_2(NH_3)_2 \rightarrow (NA)_2(NH_3)+(NH_3)$	1.28×10^3
$(NA)_2(NH_3)_2 \rightarrow (NA)_2+(NH_3)_2$	5.51×10^{-3}
$(NA)_2(NH_3)_2 \rightarrow (NA)(NH_3)_2+(NA)$	8.47×10^3
$(NA)_2(NH_3)_2 \rightarrow (NA)(NH_3)+(NA)(NH_3)$	1.22×10^8
$(NA)_2(NH_3)_3 \rightarrow (NA)_2(NH_3)_2+(NH_3)$	2.33×10^8
$(NA)_2(NH_3)_3 \rightarrow (NA)_2(NH_3)+(NH_3)_2$	7.06×10^{-2}
$(NA)_2(NH_3)_3 \rightarrow (NA)_2+(NH_3)_3$	8.66×10^{-5}
$(NA)_2(NH_3)_3 \rightarrow (NA)(NH_3)_3+(NA)$	3.59×10^2
$(NA)_2(NH_3)_3 \rightarrow (NA)(NH_3)_2+(NA)(NH_3)$	3.05×10^6
$(NA)_2(NH_3)_4 \rightarrow (NA)_2(NH_3)_3+(NH_3)$	3.67×10^3
$(NA)_2(NH_3)_4 \rightarrow (NA)_2(NH_3)_2+(NH_3)_2$	1.87×10^{-1}
$(NA)_2(NH_3)_4 \rightarrow (NA)_2(NH_3)+(NH_3)_3$	1.63×10^{-8}
$(NA)_2(NH_3)_4 \rightarrow (NA)_2+(NH_3)_4$	1.25×10^{-12}
$(NA)_2(NH_3)_4 \rightarrow (NA)(NH_3)_4+(NA)$	2.67×10^{-4}
$(NA)_2(NH_3)_4 \rightarrow (NA)(NH_3)_3+(NA)(NH_3)$	1.89
$(NA)_2(NH_3)_4 \rightarrow (NA)(NH_3)_2+(NA)(NH_3)_2$	2.79×10^{-1}
$(NA)_3 \rightarrow (NA)_2+(NA)$	2.01×10^{13}
$(NA)_3(NH_3) \rightarrow (NA)_3+(NH_3)$	2.93×10^1
$(NA)_3(NH_3) \rightarrow (NA)_2(NH_3)+(NA)$	3.30×10^7
$(NA)_3(NH_3) \rightarrow (NA)_2+(NA)(NH_3)$	9.26×10^8
$(NA)_3(NH_3)_2 \rightarrow (NA)_3(NH_3)+(NH_3)$	2.30×10^1
$(NA)_3(NH_3)_2 \rightarrow (NA)_3+(NH_3)_2$	1.50×10^{10}
$(NA)_3(NH_3)_2 \rightarrow (NA)_2(NH_3)_2+(NA)$	5.57×10^5
$(NA)_3(NH_3)_2 \rightarrow (NA)_2(NH_3)+(NA)(NH_3)$	1.11×10^3
$(NA)_3(NH_3)_2 \rightarrow (NA)_2+(NA)(NH_3)_2$	1.08
$(NA)_3(NH_3)_3 \rightarrow (NA)_3(NH_3)_2+(NH_3)$	1.37×10^5
$(NA)_3(NH_3)_3 \rightarrow (NA)_3(NH_3)+(NH_3)_2$	6.56×10^{-7}
$(NA)_3(NH_3)_3 \rightarrow (NA)_3+(NH_3)_3$	1.22×10^{-15}
$(NA)_3(NH_3)_3 \rightarrow (NA)_2(NH_3)_3+(NA)$	3.11×10^2
$(NA)_3(NH_3)_3 \rightarrow (NA)_2(NH_3)_2+(NA)(NH_3)$	1.04×10^5
$(NA)_3(NH_3)_3 \rightarrow (NA)_2(NH_3)+(NA)(NH_3)_2$	7.17×10^{-3}
$(NA)_3(NH_3)_3 \rightarrow (NA)_2+(NA)(NH_3)_3$	2.37×10^{-5}
$(NA)_3(NH_3)_4 \rightarrow (NA)_3(NH_3)_3+(NH_3)$	2.22×10^6
$(NA)_3(NH_3)_4 \rightarrow (NA)_3(NH_3)_2+(NH_3)_2$	5.93×10^{-2}
$(NA)_3(NH_3)_4 \rightarrow (NA)_3(NH_3)+(NH_3)_3$	8.13×10^{-11}
$(NA)_3(NH_3)_4 \rightarrow (NA)_3+(NH_3)_4$	9.54×10^{-21}
$(NA)_3(NH_3)_4 \rightarrow (NA)_2(NH_3)_4+(NA)$	1.78×10^5
$(NA)_3(NH_3)_4 \rightarrow (NA)_2(NH_3)_3+(NA)(NH_3)$	8.80×10^2
$(NA)_3(NH_3)_4 \rightarrow (NA)_2(NH_3)_2+(NA)(NH_3)_2$	1.02×10^1
$(NA)_3(NH_3)_4 \rightarrow (NA)_2(NH_3)+(NA)(NH_3)_3$	2.40×10^{-6}
$(NA)_3(NH_3)_4 \rightarrow (NA)_2+ (NA)(NH_3)_4$	9.50×10^{-9}
$(NA)_4 \rightarrow (NA)_3+(NA)$	8.64×10^8
$(NA)_4 \rightarrow (NA)_2+(NA)_2$	2.02×10^{12}
$(NA)_4(NH_3) \rightarrow (NA)_4+(NH_3)$	5.79×10^{-2}

Reaction	Rate
$(NA)_4(NH_3) \rightarrow (NA)_3(NH_3)+(NA)$	1.61×10^6
$(NA)_4(NH_3) \rightarrow (NA)_3+(NA)(NH_3)$	6.86×10^1
$(NA)_4(NH_3) \rightarrow (NA)_2(NH_3)+(NA)_2$	1.14×10^4
$(NA)_4(NH_3)_2 \rightarrow (NA)_4(NH_3)+(NH_3)$	2.00×10^2
$(NA)_4(NH_3)_2 \rightarrow (NA)_4+(NH_3)_2$	2.28×10^{-12}
$(NA)_4(NH_3)_2 \rightarrow (NA)_3(NH_3)_2+(NA)$	1.33×10^7
$(NA)_4(NH_3)_2 \rightarrow (NA)_3(NH_3)+(NA)(NH_3)$	4.16×10^2
$(NA)_4(NH_3)_2 \rightarrow (NA)_3+(NA)(NH_3)_2$	6.18×10^{-7}
$(NA)_4(NH_3)_2 \rightarrow (NA)_2(NH_3)_2+(NA)_2$	1.49×10^3
$(NA)_4(NH_3)_2 \rightarrow (NA)_2(NH_3)+(NA)_2(NH_3)$	5.28×10^{-2}
$(NA)_4(NH_3)_3 \rightarrow (NA)_4(NH_3)_2+(NH_3)$	1.35×10^2
$(NA)_4(NH_3)_3 \rightarrow (NA)_4(NH_3)+(NH_3)_2$	5.02×10^{-9}
$(NA)_4(NH_3)_3 \rightarrow (NA)_4+(NH_3)_3$	1.65×10^{-20}
$(NA)_4(NH_3)_3 \rightarrow (NA)_3(NH_3)_3+(NA)$	1.25×10^4
$(NA)_4(NH_3)_3 \rightarrow (NA)_3(NH_3)_2+(NA)(NH_3)$	2.19×10^3
$(NA)_4(NH_3)_3 \rightarrow (NA)_3(NH_3)+(NA)(NH_3)_2$	2.39×10^{-6}
$(NA)_4(NH_3)_3 \rightarrow (NA)_3+(NA)(NH_3)_3$	1.20×10^{-14}
$(NA)_4(NH_3)_3 \rightarrow (NA)_2(NH_3)_3+(NA)_2$	7.36×10^{-4}
$(NA)_4(NH_3)_3 \rightarrow (NA)_2(NH_3)_2+(NA)_2(NH_3)$	8.77×10^{-3}
$(NA)_4(NH_3)_4 \rightarrow (NA)_4(NH_3)_3+(NH_3)$	4.01×10^{-5}
$(NA)_4(NH_3)_4 \rightarrow (NA)_4(NH_3)_2+(NH_3)_2$	9.59×10^{-16}
$(NA)_4(NH_3)_4 \rightarrow (NA)_4(NH_3)+(NH_3)_3$	1.03×10^{-23}
$(NA)_4(NH_3)_4 \rightarrow (NA)_4+(NH_3)_4$	2.12×10^{-36}
$(NA)_4(NH_3)_4 \rightarrow (NA)_3(NH_3)_4+(NA)$	2.17×10^{-7}
$(NA)_4(NH_3)_4 \rightarrow (NA)_3(NH_3)_3+(NA)(NH_3)$	5.83×10^{-7}
$(NA)_4(NH_3)_4 \rightarrow (NA)_3(NH_3)_2+(NA)(NH_3)_2$	3.57×10^{-12}
$(NA)_4(NH_3)_4 \rightarrow (NA)_3(NH_3)+(NA)(NH_3)_3$	1.32×10^{-20}
$(NA)_4(NH_3)_4 \rightarrow (NA)_3+(NA)(NH_3)_4$	7.97×10^{-29}
$(NA)_4(NH_3)_4 \rightarrow (NA)_2(NH_3)_4+(NA)_2$	6.98×10^{-12}
$(NA)_4(NH_3)_4 \rightarrow (NA)_2(NH_3)_3+(NA)_2(NH_3)$	1.23×10^{-15}
$(NA)_4(NH_3)_4 \rightarrow (NA)_2(NH_3)_2+(NA)_2(NH_3)_2$	1.04×10^{-10}
$(MA)_2 \rightarrow (MA)+(MA)$	4.53×10^{12}
$(MA)_3 \rightarrow (MA)_2+(MA)$	4.96×10^{10}
$(MA)_4 \rightarrow (MA)_3+(MA)$	3.81×10^{11}
$(MA)_4 \rightarrow (MA)_2 +(MA)_2$	8.69×10^8
$(NA)(MA) \rightarrow (NA)+(MA)$	3.91×10^5
$(NA)(MA)_2 \rightarrow (NA)(MA)+(MA)$	6.71×10^{10}
$(NA)(MA)_2 \rightarrow (NA)+(MA)_2$	2.95×10^3
$(NA)(MA)_3 \rightarrow (NA)(MA)_2+(MA)$	1.61×10^9
$(NA)(MA)_3 \rightarrow (NA)(MA)+(MA)_2$	1.01×10^7
$(NA)(MA)_3 \rightarrow (NA)+(MA)_3$	9.71×10^1
$(NA)(MA)_4 \rightarrow (NA)(MA)_3 +(MA)$	5.21×10^{10}
$(NA)(MA)_4 \rightarrow (NA)(MA)_2 +(MA)_2$	6.85×10^6
$(NA)(MA)_4 \rightarrow (NA)(MA)+(MA)_3$	9.37×10^6

23

$(NA)(MA)_4 \rightarrow (NA)+(MA)_4$	1.34×10^1
$(NA)_2(MA) \rightarrow (NA)_2+(MA)$	4.70×10^5
$(NA)_2(MA) \rightarrow (NA)(MA)+(NA)$	4.56×10^9
$(NA)_2(MA)_2 \rightarrow (NA)_2(MA)+(MA)$	1.01×10^{-1}
$(NA)_2(MA)_2 \rightarrow (NA)_2+(MA)_2$	4.49×10^{-9}
$(NA)_2(MA)_2 \rightarrow (NA)(MA)_2+(NA)$	6.97×10^{-3}
$(NA)_2(MA)_2 \rightarrow (NA)(MA)+(NA)(MA)$	4.95×10^2
$(NA)_2(MA)_3 \rightarrow (NA)_2(MA)_2+(MA)$	3.25×10^6
$(NA)_2(MA)_3 \rightarrow (NA)_2(MA)+(MA)_2$	2.70×10^{-8}
$(NA)_2(MA)_3 \rightarrow (NA)_2+(MA)_3$	2.63×10^{-13}
$(NA)_2(MA)_3 \rightarrow (NA)(MA)_3+(NA)$	1.42×10^{-5}
$(NA)_2(MA)_3 \rightarrow (NA)(MA)_2+(NA)(MA)$	4.24×10^{-2}
$(NA)_2(MA)_4 \rightarrow (NA)_2(MA)_3+(MA)$	4.63×10^7
$(NA)_2(MA)_4 \rightarrow (NA)_2(MA)_2+(MA)_2$	1.11×10^1
$(NA)_2(MA)_4 \rightarrow (NA)_2(MA)+(MA)_3$	2.03×10^{-11}
$(NA)_2(MA)_4 \rightarrow (NA)_2+(MA)_4$	2.93×10^{-17}
$(NA)_2(MA)_4 \rightarrow (NA)(MA)_4+(NA)$	1.27×10^{-8}
$(NA)_2(MA)_4 \rightarrow (NA)(MA)_3+(NA)(MA)$	1.10×10^{-3}
$(NA)_2(MA)_4 \rightarrow (NA)(MA)_2+(NA)(MA)_2$	1.16×10^{-5}
$(NA)_3(MA) \rightarrow (NA)_3+(MA)$	1.79
$(NA)_3(MA) \rightarrow (NA)_2(MA)+(NA)$	4.54×10^7
$(NA)_3(MA) \rightarrow (NA)_2+(NA)(MA)$	4.59×10^7
$(NA)_3(MA)_2 \rightarrow (NA)_3(MA)+(MA)$	1.23×10^{-1}
$(NA)_3(MA)_2 \rightarrow (NA)_3+(MA)_2$	1.84×10^{-14}
$(NA)_3(MA)_2 \rightarrow (NA)_2(MA)_2+(NA)$	5.61×10^7
$(NA)_3(MA)_2 \rightarrow (NA)_2(MA)+(NA)(MA)$	1.06×10^1
$(NA)_3(MA)_2 \rightarrow (NA)_2+(NA)(MA)_2$	7.54×10^{-5}
$(NA)_3(MA)_3 \rightarrow (NA)_3(MA)_2+(MA)$	2.86×10^{-1}
$(NA)_3(MA)_3 \rightarrow (NA)_3(MA)+(MA)_2$	2.63×10^{-15}
$(NA)_3(MA)_3 \rightarrow (NA)_3+(MA)_3$	8.62×10^{-26}
$(NA)_3(MA)_3 \rightarrow (NA)_2(MA)_3+(NA)$	4.98
$(NA)_3(MA)_3 \rightarrow (NA)_2(MA)_2+(NA)(MA)$	2.72×10^1
$(NA)_3(MA)_3 \rightarrow (NA)_2(MA)+(NA)(MA)_2$	3.62×10^{-11}
$(NA)_3(MA)_3 \rightarrow (NA)_2+(NA)(MA)_3$	1.22×10^{-14}
$(NA)_3(MA)_4 \rightarrow (NA)_3(MA)_3+(MA)$	1.99×10^6
$(NA)_3(MA)_4 \rightarrow (NA)_3(MA)_2+(MA)_2$	3.87×10^{-8}
$(NA)_3(MA)_4 \rightarrow (NA)_3(MA)+(MA)_3$	7.83×10^{-20}
$(NA)_3(MA)_4 \rightarrow (NA)_3+ (MA)_4$	3.81×10^{-31}
$(NA)_3(MA)_4 \rightarrow (NA)_2(MA)_4+(NA)$	2.15×10^{-1}
$(NA)_3(MA)_4 \rightarrow (NA)_2(MA)_3+(NA)(MA)$	1.53×10^1
$(NA)_3(MA)_4 \rightarrow (NA)_2(MA)_2+(NA)(MA)_2$	5.91×10^{-4}
$(NA)_3(MA)_4 \rightarrow (NA)_2(MA)+(NA)(MA)_3$	3.74×10^{-14}
$(NA)_3(MA)_4 \rightarrow (NA)_2+(NA)(MA)_4$	4.34×10^{-19}
$(NA)_4(MA) \rightarrow (NA)_4+(MA)$	2.87×10^2

$(NA)_4(MA) \rightarrow (NA)_3(MA)+(NA)$	1.61×10^{11}
$(NA)_4(MA) \rightarrow (NA)_3+(NA)(MA)$	5.46×10^5
$(NA)_4(MA) \rightarrow (NA)_2(MA)+(NA)_2$	1.42×10^9
$(NA)_4(MA)_2 \rightarrow (NA)_4(MA)+(MA)$	5.64×10^{-6}
$(NA)_4(MA)_2 \rightarrow (NA)_4+(MA)_2$	1.22×10^{-16}
$(NA)_4(MA)_2 \rightarrow (NA)_3(MA)_2+(NA)$	7.42×10^6
$(NA)_4(MA)_2 \rightarrow (NA)_3(MA)+(NA)(MA)$	1.55
$(NA)_4(MA)_2 \rightarrow (NA)_3+(NA)(MA)_2$	3.72×10^{-11}
$(NA)_4(MA)_2 \rightarrow (NA)_2(MA)_2+(NA)_2$	7.28×10^4
$(NA)_4(MA)_2 \rightarrow (NA)_2(MA)+(NA)_2(MA)$	6.81×10^{-3}
$(NA)_4(MA)_3 \rightarrow (NA)_4(MA)_2+(MA)$	1.96×10^1
$(NA)_4(MA)_3 \rightarrow (NA)_4(MA)+(MA)_2$	7.60×10^{-18}
$(NA)_4(MA)_3 \rightarrow (NA)_4+(MA)_3$	3.61×10^{-26}
$(NA)_4(MA)_3 \rightarrow (NA)_3(MA)_3+(NA)$	5.13×10^8
$(NA)_4(MA)_3 \rightarrow (NA)_3(MA)_2+(NA)(MA)$	2.27×10^2
$(NA)_4(MA)_3 \rightarrow (NA)_3(MA)+(NA)(MA)_2$	3.36×10^{-10}
$(NA)_4(MA)_3 \rightarrow (NA)_3+(NA)(MA)_3$	3.81×10^{-19}
$(NA)_4(MA)_3 \rightarrow (NA)_2(MA)_3+(NA)_2$	4.07×10^{-1}
$(NA)_4(MA)_3 \rightarrow (NA)_2(MA)_2+(NA)_2(MA)$	2.21
$(NA)_4(MA)_4 \rightarrow (NA)_4(MA)_3+(MA)$	3.47×10^{-7}
$(NA)_4(MA)_4 \rightarrow (NA)_4(MA)_2+(MA)_2$	4.32×10^{-19}
$(NA)_4(MA)_4 \rightarrow (NA)_4(MA)+(MA)_3$	3.69×10^{-35}
$(NA)_4(MA)_4 \rightarrow (NA)_4 +(MA)_4$	2.60×10^{-44}
$(NA)_4(MA)_4 \rightarrow (NA)_3(MA)_4+(NA)$	9.02×10^{-5}
$(NA)_4(MA)_4 \rightarrow (NA)_3(MA)_3+(NA)(MA)$	2.57×10^{-4}
$(NA)_4(MA)_4 \rightarrow (NA)_3(MA)_2+(NA)(MA)_2$	8.05×10^{-16}
$(NA)_4(MA)_4 \rightarrow (NA)_3(MA)+(NA)(MA)_3$	5.66×10^{-26}
$(NA)_4(MA)_4 \rightarrow (NA)_3+(NA)(MA)_4$	2.20×10^{-36}
$(NA)_4(MA)_4 \rightarrow (NA)_2(MA)_4+(NA)_2$	2.87×10^{-15}
$(NA)_4(MA)_4 \rightarrow (NA)_2(MA)_3+(NA)_2(MA)$	2.03×10^{-13}
$(NA)_4(MA)_4 \rightarrow (NA)_2(MA)_2+(NA)_2(MA)_2$	2.94×10^{-6}
$(DMA)_2 \rightarrow (DMA)+(DMA)$	7.77×10^{13}
$(DMA)_3 \rightarrow (DMA)_2+(DMA)$	1.95×10^{10}
$(DMA)_4 \rightarrow (DMA)_3+(DMA)$	2.10×10^{12}
$(DMA)_4 \rightarrow (DMA)_2+(DMA)_2$	1.10×10^8
$(NA)(DMA) \rightarrow (NA)+(DMA)$	7.23×10^4
$(NA)(DMA)_2 \rightarrow (NA)(DMA)+(DMA)$	1.69×10^9
$(NA)(DMA)_2 \rightarrow (NA)+(DMA)_2$	8.53×10^{-1}
$(NA)(DMA)_3 \rightarrow (NA)(DMA)_2 +(DMA)$	7.31×10^9
$(NA)(DMA)_3 \rightarrow (NA)(DMA)+(DMA)_2$	6.99×10^4
$(NA)(DMA)_3 \rightarrow (NA)+(DMA)_3$	3.38×10^{-1}
$(NA)(DMA)_4 \rightarrow (NA)(DMA)_3 +(DMA)$	4.17×10^{10}
$(NA)(DMA)_4 \rightarrow (NA)(DMA)_2 +(DMA)_2$	1.49×10^6
$(NA)(DMA)_4 \rightarrow (NA)(DMA)+(DMA)_3$	1.36×10^5

$(NA)(DMA)_4 \rightarrow (NA)+(DMA)_4$	7.00×10^{-3}
$(NA)_2(DMA) \rightarrow (NA)_2+(DMA)$	1.01×10^1
$(NA)_2(DMA) \rightarrow (NA)(DMA)+(NA)$	5.53×10^5
$(NA)_2(DMA)_2 \rightarrow (NA)_2(DMA)+(DMA)$	7.24×10^{-5}
$(NA)_2(DMA)_2 \rightarrow (NA)_2+(DMA)_2$	4.37×10^{-18}
$(NA)_2(DMA)_2 \rightarrow (NA)(DMA)_2+(NA)$	2.51×10^{-8}
$(NA)_2(DMA)_2 \rightarrow (NA)(DMA)+(NA)(DMA)$	2.38×10^{-4}
$(NA)_2(DMA)_3 \rightarrow (NA)_2(DMA)_2+(DMA)$	1.33×10^{11}
$(NA)_2(DMA)_3 \rightarrow (NA)_2(DMA)+(DMA)_2$	4.90×10^{-8}
$(NA)_2(DMA)_3 \rightarrow (NA)_2+(DMA)_3$	2.83×10^{-17}
$(NA)_2(DMA)_3 \rightarrow (NA)(DMA)_3+(NA)$	4.76×10^{-7}
$(NA)_2(DMA)_3 \rightarrow (NA)(DMA)_2+(NA)(DMA)$	3.37×10^{-2}
$(NA)_2(DMA)_4 \rightarrow (NA)_2(DMA)_3+(DMA)$	6.49×10^8
$(NA)_2(DMA)_4 \rightarrow (NA)_2(DMA)_2+(DMA)_2$	3.90×10^5
$(NA)_2(DMA)_4 \rightarrow (NA)_2(DMA)+(DMA)_3$	1.38×10^{-9}
$(NA)_2(DMA)_4 \rightarrow (NA)_2+(DMA)_4$	8.44×10^{-21}
$(NA)_2(DMA)_4 \rightarrow (NA)(DMA)_4+(NA)$	7.69×10^{-9}
$(NA)_2(DMA)_4 \rightarrow (NA)(DMA)_3+(NA)(DMA)$	2.77×10^{-3}
$(NA)_2(DMA)_4 \rightarrow (NA)(DMA)_2+(NA)(DMA)_2$	5.19×10^{-3}
$(NA)_3(DMA) \rightarrow (NA)_3+(DMA)$	1.49×10^{-2}
$(NA)_3(DMA) \rightarrow (NA)_2(DMA)+(NA)$	3.19×10^{10}
$(NA)_3(DMA) \rightarrow (NA)_2+(NA)(DMA)$	3.81×10^6
$(NA)_3(DMA)_2 \rightarrow (NA)_3(DMA)+(DMA)$	2.53×10^{-7}
$(NA)_3(DMA)_2 \rightarrow (NA)_3+(DMA)_2$	2.02×10^{-23}
$(NA)_3(DMA)_2 \rightarrow (NA)_2(DMA)_2+(NA)$	1.17×10^8
$(NA)_3(DMA)_2 \rightarrow (NA)_2(DMA)+(NA)(DMA)$	8.56×10^{-2}
$(NA)_3(DMA)_2 \rightarrow (NA)_2+(NA)(DMA)_2$	5.41×10^{-10}
$(NA)_3(DMA)_3 \rightarrow (NA)_3(DMA)_2+(DMA)$	1.45×10^1
$(NA)_3(DMA)_3 \rightarrow (NA)_3(DMA)+(DMA)_2$	1.73×10^{-20}
$(NA)_3(DMA)_3 \rightarrow (NA)_3+(DMA)_3$	1.32×10^{-32}
$(NA)_3(DMA)_3 \rightarrow (NA)_2(DMA)_3+(NA)$	1.33×10^{-2}
$(NA)_3(DMA)_3 \rightarrow (NA)_2(DMA)_2+(NA)(DMA)$	1.58×10^4
$(NA)_3(DMA)_3 \rightarrow (NA)_2(DMA)+(NA)(DMA)_2$	6.12×10^{-10}
$(NA)_3(DMA)_3 \rightarrow (NA)_2+(NA)(DMA)_3$	1.03×10^{-18}
$(NA)_3(DMA)_4 \rightarrow (NA)_3(DMA)_3+(DMA)$	3.92×10^8
$(NA)_3(DMA)_4 \rightarrow (NA)_3(DMA)_2+(DMA)_2$	2.41×10^{-5}
$(NA)_3(DMA)_4 \rightarrow (NA)_3(DMA)+(DMA)_3$	2.75×10^{-22}
$(NA)_3(DMA)_4 \rightarrow (NA)_3+(DMA)_4$	2.22×10^{-36}
$(NA)_3(DMA)_4 \rightarrow (NA)_2(DMA)_4+(NA)$	8.31×10^{-3}
$(NA)_3(DMA)_4 \rightarrow (NA)_2(DMA)_3+(NA)(DMA)$	4.37×10^1
$(NA)_3(DMA)_4 \rightarrow (NA)_2(DMA)_2+(NA)(DMA)_2$	2.75×10^3
$(NA)_3(DMA)_4 \rightarrow (NA)_2(DMA)+(NA)(DMA)_3$	2.84×10^{-11}
$(NA)_3(DMA)_4 \rightarrow (NA)_2+(NA)(DMA)_4$	9.39×10^{-21}
$(NA)_4(DMA) \rightarrow (NA)_4+(DMA)$	8.21×10^{-3}

$(NA)_4(DMA) \rightarrow (NA)_3(DMA)+(NA)$	5.03×10^8
$(NA)_4(DMA) \rightarrow (NA)_3+(NA)(DMA)$	7.93×10^1
$(NA)_4(DMA) \rightarrow (NA)_2(DMA)+(NA)_2$	3.09×10^9
$(NA)_4(DMA)_2 \rightarrow (NA)_4(DMA)+(DMA)$	6.67×10^{-8}
$(NA)_4(DMA)_2 \rightarrow (NA)_4+(DMA)_2$	2.68×10^{-24}
$(NA)_4(DMA)_2 \rightarrow (NA)_3(DMA)_2+(NA)$	1.38×10^8
$(NA)_4(DMA)_2 \rightarrow (NA)_3(DMA)+(NA)(DMA)$	3.25×10^{-4}
$(NA)_4(DMA)_2 \rightarrow (NA)_3+(NA)(DMA)_2$	2.71×10^{-15}
$(NA)_4(DMA)_2 \rightarrow (NA)_2(DMA)_2+(NA)_2$	2.73×10^6
$(NA)_4(DMA)_2 \rightarrow (NA)_2(DMA)+(NA)_2(DMA)$	0.84×10^1
$(NA)_4(DMA)_3 \rightarrow (NA)_4(DMA)_2+(DMA)$	6.94×10^{-1}
$(NA)_4(DMA)_3 \rightarrow (NA)_4(DMA)+(DMA)_2$	2.03×10^{-22}
$(NA)_4(DMA)_3 \rightarrow (NA)_4+(DMA)_3$	7.78×10^{-35}
$(NA)_4(DMA)_3 \rightarrow (NA)_3(DMA)_3+(NA)$	6.82×10^6
$(NA)_4(DMA)_3 \rightarrow (NA)_3(DMA)_2+(NA)(DMA)$	8.27×10^2
$(NA)_4(DMA)_3 \rightarrow (NA)_3(DMA)+(NA)(DMA)_2$	1.03×10^{-13}
$(NA)_4(DMA)_3 \rightarrow (NA)_3+ (NA)(DMA)_3$	2.30×10^{-25}
$(NA)_4(DMA)_3 \rightarrow (NA)_2(DMA)_3+(NA)_2$	1.38×10^{-5}
$(NA)_4(DMA)_3 \rightarrow (NA)_2(DMA)_2+(NA)_2(DMA)$	1.37×10^5
$(NA)_4(DMA)_4 \rightarrow (NA)_4(DMA)_3+(DMA)$	5.88×10^{-6}
$(NA)_4(DMA)_4 \rightarrow (NA)_4(DMA)_2+(DMA)_2$	1.63×10^{-20}
$(NA)_4(DMA)_4 \rightarrow (NA)_4(DMA)+(DMA)_3$	4.57×10^{-38}
$(NA)_4(DMA)_4 \rightarrow (NA)_4+(DMA)_4$	1.86×10^{-52}
$(NA)_4(DMA)_4 \rightarrow (NA)_3(DMA)_4+(NA)$	1.05×10^{-7}
$(NA)_4(DMA)_4 \rightarrow (NA)_3(DMA)_3+(NA)(DMA)$	3.16×10^{-4}
$(NA)_4(DMA)_4 \rightarrow (NA)_3(DMA)_2+(NA)(DMA)_2$	2.04×10^{-12}
$(NA)_4(DMA)_4 \rightarrow (NA)_3(DMA)+(NA)(DMA)_3$	6.80×10^{-29}
$(NA)_4(DMA)_4 \rightarrow (NA)_3+(NA)(DMA)_4$	2.96×10^{-41}
$(NA)_4(DMA)_4 \rightarrow (NA)_2(DMA)_4+(NA)_2$	1.21×10^{-19}
$(NA)_4(DMA)_4 \rightarrow (NA)_2(DMA)_3+(NA)_2(DMA)$	5.38×10^{-12}
$(NA)_4(DMA)_4 \rightarrow (NA)_2(DMA)_2+(NA)_2(DMA)_2$	4.38×10^3

282

283 **Table S5.** Calculated Gibbs free energy of stepwise hydration for $(NA)_m(R_1NHR_2)_n$ ($0 \leq m$, $n \leq 2$)

284 at the DLPNO-CCSD(T)/aug-cc-pVTZ//M06-2X/6-31++G(d,p) level of theory, and 298.15 K and

285 1 atm.

Cluster	n (H_2O)							
	n = 1	n = 2	n = 3	n = 4	n = 5	n = 6	n = 7	n = 8
NA	-2.45	-2.39	-1.73					
$(NA)_2$	-1.19	-2.49	-1.11					
NH_3	-0.11	-1.84	-3.12					
$(NH_3)_2$	-2.11	-2.05	-1.48					
$(NA)(NH_3)$	0.01	-1.51	-2.64	-9.02	-2.65			

(NA)(NH$_3$)$_2$	0.05	-3.04	-2.86	-5.51	-0.05			
(NA)$_2$(NH$_3$)	-3.69	-3.66	-7.48	-0.21	-2.41			
(NA)$_2$(NH$_3$)$_2$	-4.46	-4.15	-3.91	-7.8	-4.86	-2.18	-5.11	0.29
MA	-0.21	-1.43	-1.86	-0.88				
(MA)$_2$	-2.66	-1.32	-1.86	1.46				
(NA)(MA)	-0.59	-3.26	-6.01	-6.37	-5.93	-2.13	-1.54	
(NA)(MA)$_2$	-4.23	-5.24	-4.8	0.22				
(NA)$_2$(MA)	-4.20	-1.66	-7.75	0.86				
(NA)$_2$(MA)$_2$	-5.97	-3.01	-6.21	2.58				
DMA	-0.41	-1.07	-2.77	-1.59				
(DMA)$_2$	-2.32	-3.81	-3.81	-1.51				
(NA)(DMA)	-2.81	-5.47	-5.19	5.96				
(NA)(DMA)$_2$	-4.64	-5.29	-5.4	1.66				
(NA)$_2$(DMA)	-1.41	-5.41	-2.51	-2.07	-6.19	-2.21	-0.87	
(NA)$_2$(DMA)$_2$	-1.24	-1.66	-4.8	2.78				

286

287 **Table S6.** Thermodynamical quantities ΔH (kcal/mol) and ΔS (cal/(mol·K)) of stepwise hydration

288 for (NA)$_m$(R$_1$NHR$_2$)$_n$(W)$_x$ (x = 1 ~ 8) clusters under study at 298.15 K and 1 atm.

Cluster	ΔH	ΔS
(NA)(W)	-11.21	-31.5
(NA)(W)$_2$	-22.62	-63.9
(NA)(W)$_3$	-33.39	-96.4
(NA)$_2$(W)	-20.00	-66.4
(NA)$_2$(W)$_2$	-32.48	-102.3
(NA)$_2$(W)$_3$	-44.87	-142.9
(NH$_3$)(W)	-7.67	-27.2
(NH$_3$)(W)$_2$	-18.79	-60.5
(NH$_3$)(W)$_3$	-31.24	-94.1
(NH$_3$)$_2$(W)	-16.30	-59.4
(NH$_3$)$_2$(W)$_2$	-27.56	-90.9
(NH$_3$)$_2$(W)$_3$	-39.56	-128.7
(NA)(NH$_3$)(W)	-25.17	-64.7
(NA)(NH$_3$)(W)$_2$	-37.01	-101.8
(NA)(NH$_3$)(W)$_3$	-48.93	-135.2
(NA)(NH$_3$)(W)$_4$	-68.18	-172.0
(NA)(NH$_3$)(W)$_5$	-75.87	-209.2
(NA)(NH$_3$)$_2$(W)	-36.39	-105.4
(NA)(NH$_3$)$_2$(W)$_2$	-49.31	-140.9
(NA)(NH$_3$)$_2$(W)$_3$	-60.71	-171.6
(NA)(NH$_3$)$_2$(W)$_4$	-76.80	-209.6
(NA)(NH$_3$)$_2$(W)$_5$	-87.60	-248.3
(NA)$_2$(NH$_3$)(W)	-40.24	-107.3

(NA)$_2$(NH$_3$)(W)$_2$	-53.49	-141.8
(NA)$_2$(NH$_3$)(W)$_3$	-71.93	-181.2
(NA)$_2$(NH$_3$)(W)$_4$	-82.14	-217.1
(NA)$_2$(NH$_3$)(W)$_5$	-95.93	-258.1
(NA)$_2$(NH$_3$)$_2$(W)	-62.64	-145.1
(NA)$_2$(NH$_3$)$_2$(W)$_2$	-76.31	-179.3
(NA)$_2$(NH$_3$)$_2$(W)$_3$	-90.29	-215.5
(NA)$_2$(NH$_3$)$_2$(W)$_4$	-108.95	-254.6
(NA)$_2$(NH$_3$)$_2$(W)$_5$	-123.29	-288.7
(NA)$_2$(NH$_3$)$_2$(W)$_6$	-133.23	-316.6
(NA)$_2$(NH$_3$)$_2$(W)$_7$	-147.68	-350.2
(NA)$_2$(NH$_3$)$_2$(W)$_8$	-160.59	-397.7
(MA)(W)	-8.18	-28.7
(MA)(W)$_2$	-18.95	-61.5
(MA)(W)$_3$	-31.35	-95.7
(MA)$_2$(W)	-16.51	-63.4
(MA)$_2$(W)$_2$	-28.57	-93.9
(MA)$_2$(W)$_3$	-41.24	-132.8
(NA)(MA)(W)	-27.90	-67.8
(NA)(MA)(W)$_2$	-42.22	-107.5
(NA)(MA)(W)$_3$	-56.78	-138.3
(NA)(MA)(W)$_4$	-72.44	-171.7
(NA)(MA)(W)$_5$	-88.53	-208.2
(NA)(MA)(W)$_6$	-100.56	-243.8
(NA)(MA)(W)$_7$	-112.26	-280.3
(NA)(MA)$_2$(W)	-42.29	-107.7
(NA)(MA)$_2$(W)$_2$	-57.08	-141.8
(NA)(MA)$_2$(W)$_3$	-71.90	-178.1
(NA)(MA)$_2$(W)$_4$	-80.91	-211.3
(NA)$_2$(MA)(W)	-46.50	-111.6
(NA)$_2$(MA)(W)$_2$	-58.81	-149.9
(NA)$_2$(MA)(W)$_3$	-75.94	-183.6
(NA)$_2$(MA)(W)$_4$	-84.28	-216.7
(NA)$_2$(MA)$_2$(W)	-73.98	-147.0
(NA)$_2$(MA)$_2$(W)$_2$	-86.78	-182.2
(NA)$_2$(MA)$_2$(W)$_3$	-98.39	-201.6
(NA)$_2$(MA)$_2$(W)$_4$	-109.75	-251.7
(DMA)(W)	-8.43	-28.8
(DMA)(W)$_2$	-19.18	-63.6
(DMA)(W)$_3$	-30.61	-94.8
(DMA)$_2$(W)	-14.57	-62.1
(DMA)$_2$(W)$_2$	-28.06	-97.0
(DMA)$_2$(W)$_3$	-41.08	-130.1
(NA)(DMA)(W)	-30.72	-67.7

(NA)(DMA)(W)$_2$	-45.69	-101.8
(NA)(DMA)(W)$_3$	-60.75	-137.3
(NA)(DMA)(W)$_4$	-63.97	-170.3
(NA)(DMA)$_2$(W)	-45.32	-104.9
(NA)(DMA)$_2$(W)$_2$	-60.47	-140.4
(NA)(DMA)$_2$(W)$_3$	-75.72	-175.8
(NA)(DMA)$_2$(W)$_4$	-84.12	-211.9
(NA)$_2$(DMA)(W)	-49.67	-111.8
(NA)$_2$(DMA)(W)$_2$	-64.47	-145.6
(NA)$_2$(DMA)(W)$_3$	-77.61	-183.8
(NA)$_2$(DMA)(W)$_4$	-88.27	-214.7
(NA)$_2$(DMA)(W)$_5$	-105.14	-253.0
(NA)$_2$(DMA)(W)$_6$	-118.30	-292.4
(NA)$_2$(DMA)(W)$_7$	-126.24	-317.9
(NA)$_2$(DMA)$_2$(W)	-79.68	-150.9
(NA)$_2$(DMA)$_2$(W)$_2$	-90.43	-183.6
(NA)$_2$(DMA)$_2$(W)$_3$	-104.80	-218.1
(NA)$_2$(DMA)$_2$(W)$_4$	-112.51	-255.8

289

References

291 1.   Ortega, I. K.; Kupiainen, O.; Kurten, T.; Olenius, T.; Wilkman, O.; McGrath, M. J.; Loukonen, V.;
292 Vehkamaki, H., From quantum chemical formation free energies to evaporation rates. *Atmos. Chem.*
293 *Phys.* **2012,** *12* (1), 225-235.

294 2.   Chapman, S.; Cowling, T. G., *The Mathematical Theory of Nonuniform Gases: An Account of the*
295 *Kinetic Theory of Viscosity, Thermal Conduction and Diffusion in Gases*. Cambridge University Press:
296 **1970**.

297 3.   Bader, R. F. W., *Atoms in Molecules: A Quantum Theory*. Oxford University Press: Oxford, UK,
298 **1990**.

299 4.   Duarte, D. J. R.; Sosa, G. L.; Peruchena, N. M., Nature of halogen bonding. A study based on the
300 topological analysis of the Laplacian of the electron charge density and an energy decomposition
301 analysis. *Journal of Molecular Modeling* **2013,** *19* (5), 2035-2041.

302 5.   Huang, R.; Du, R.; Liu, G.; Zhao, X.; Ye, S.; Wu, G., A combined experimental and theoretical
303 approach to the study of hydrogen bond interaction in the binary mixture of N-methylimidazole with
304 water. *The Journal of Chemical Thermodynamics* **2012,** *55*, 60-66.

305 6.   Zeng, Y.; Zhang, X.; Li, X.; Zheng, S.; Meng, L., Ab initio and AIM studies on typical π-type and
306 pseudo-π-type halogen bonds: Comparison with hydrogen bonds. *International Journal of Quantum*
307 *Chemistry* **2011,** *111* (14), 3725-3740.

308 7.   Johnson, E. R.; Keinan, S.; Mori-Sánchez, P.; Contreras-García, J.; Cohen, A. J.; Yang, W.,
309 Revealing Noncovalent Interactions. *Journal of the American Chemical Society* **2010,** *132* (18), 6498-
310 6506.

311 8.   Amezaga, N. J. M.; Pamies, S. C.; Peruchena, N. M.; Sosa, G. L., Halogen Bonding: A Study
312 based on the Electronic Charge Density. *The Journal of Physical Chemistry A* **2010,** *114* (1), 552-562.

313 9.   Politzer, P.; Murray, J. S.; Clark, T., Halogen bonding: an electrostatically-driven highly

314   directional noncovalent interaction. *Phys. Chem. Chem. Phys.* **2010,** *12* (28), 7748-7757.

315   10.   Bone, R. G. A.; Bader, R. F. W., Identifying and Analyzing Intermolecular Bonding Interactions

316   in van der Waals Molecules. *The Journal of Physical Chemistry* **1996,** *100* (26), 10892-10911.

317   11.   Cremer, D.; Kraka, E., Chemical Bonds without Bonding Electron Density — Does the

318   Difference Electron-Density Analysis Suffice for a Description of the Chemical Bond? *Angewandte*

319   *Chemie International Edition in English* **1984,** *23* (8), 627-628.

320   12.   Lu, T.; Chen, F., http://sobereva.com/multiwfn/. *J. Comput. Chem.* **2012,** *33*, 580-592.

321   13.   Humphrey, W.; Dalke, A.; Schulten, K., VMD: Visual molecular dynamics. *Journal of Molecular*

322   *Graphics* **1996,** *14* (1), 33-38.

323   14.   Foster, J. P.; Weinhold, F., Natural hybrid orbitals. *J. Am. Chem. Soc.* **1980,** *102* (24), 7211-7218.

324   15.   Reed, A. E.; Weinhold, F., Natural bond orbital analysis of near-Hartree–Fock water dimer. *J.*

325   *Chem. Phys.* **1983,** *78* (6), 4066-4073.